The 9th International Symposium on Non-equilibrium Dynamics (NeD-2022)
28 Nov.--2 Dec. 2022 Krabi, Thailand.

Effects of a phase transition on two-pion interferometry in heavy-ion collisions at $\sqrt{s_{NN}} = 2.4 - 7.7$ GeV

Pengcheng Li

Institut für Theoretische Physik, Johann Wolfgang Goethe Universität Frankfurt,
Frankfurt am Main 60438, Germany
School of Science, Huzhou University, Huzhou 313000, China
School of Nuclear Science and Technology, Lanzhou University, Lanzhou 730000, China

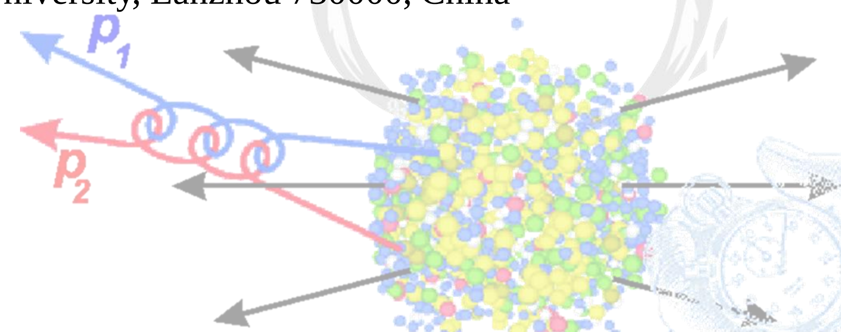

In collaboration with J. Steinheimer, T. Reichert, A. Kittiratpattana, M. Bleicher, Q. F. Li

Based on: arXiv 2209.01413 [nucl-th], accepted by Sci. China-Phys. Mech. Astron.

GOETHE UNIVERSITÄT FRANKFURT AM MAIN

蘭州大學 LANZHOU UNIVERSITY

湖州師範學院 Huzhou University

Outline

1. HBT interferometry and Motivation

2. UrQMD model

3. Results and Discussion

    1) EoS without phase transitions

    2) EoS with phase transitions

4. Summary & Outlook

The origin of HBT interferometry

Robert Hanbury-Brown and Richard Q. Twiss (HBT) interferometry
(also known as two-identical particle correlation, femtoscopy)

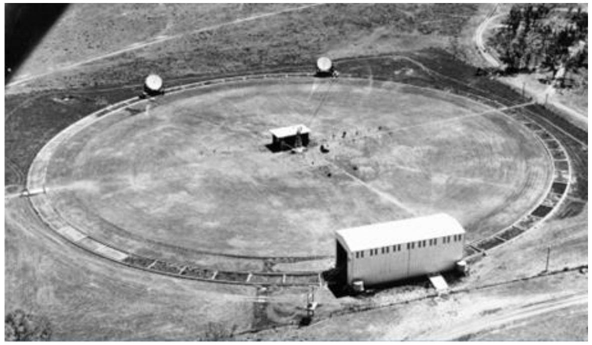

Idealized in the 1950's by Robert Hanbury-Brown, as a means to measure stellar radii through the angle subtended by nearby stars, as seen from the Earth's surface.

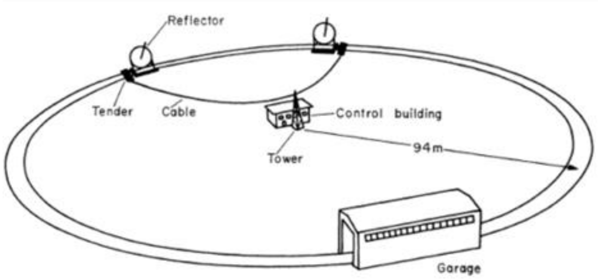

Before performing the experiment, Hanbury-Brown invited Richard Q. Twiss to develop the mathematical theory of intensity interference (second-order interference). R. Hanbury Brown and R. Q. Twiss Phil. Mag. 45, 663 (1954), Nature 177, 27–29 (1956) ; 178, 1447 (1956).

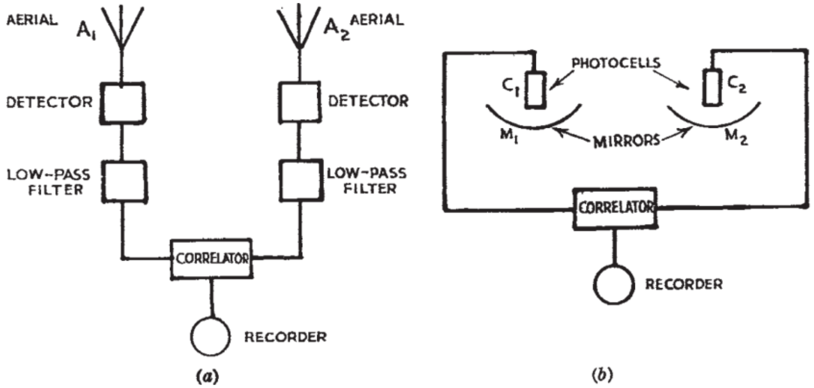

In 1956, Purcell found that photons tended to arrive in pairs at the two mirrors, as a consequence of Bose-Einstein statistics. E. M. Purcell, Nature 178, 1449 (1956).

The development of HBT interferometry

In 1959, Goldhaber, Goldhaber, Lee and Pais performed $p + \bar{p}$@1.05 GeV/c at the Bevalac/LBL, aiming at the discovery of the ρ_0 resonance ($\rho_0 \rightarrow \pi^+\pi^-$). They observed an unexpected angular correlation among identical pions (GGLP effect)! Phys. Rev. Lett. 3, 181-183 (1959).

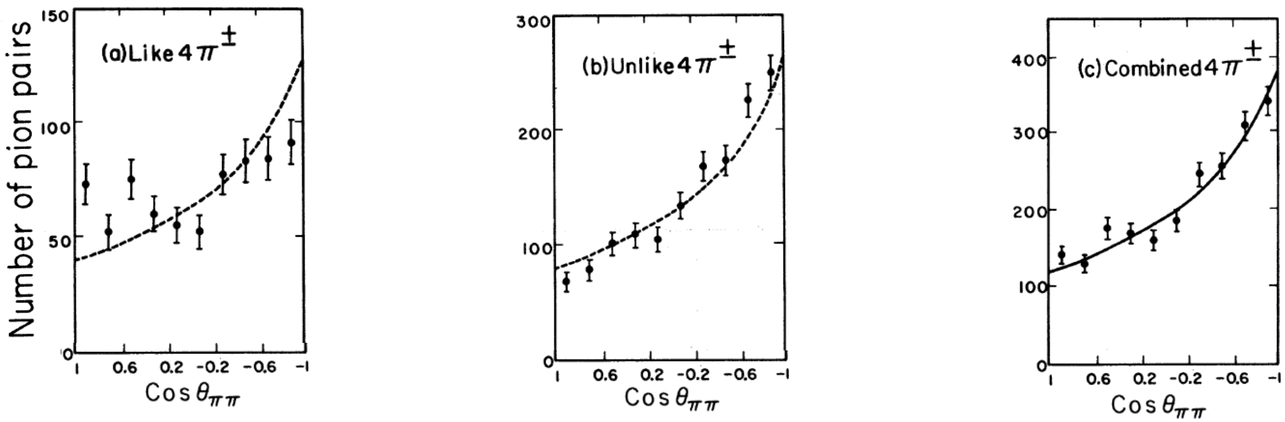

In 1960, they successfully reproduced the empirical angular distribution by a detailed multi-π phase-space calculation using symmetrized wave functions for particles of like charge. They concluded the effect was a consequence of the Bose-Einstein nature of $\pi^+\pi^+$ and $\pi^-\pi^-$, and parameterized the observed correlation as:

$$C(Q^2)=1+e^{-Q^2R^2}=1+e^{(q_0-\mathbf{q}^2)R^2}.$$

"…the dependence of angular correlation effects on the value of the radius is rather sensitive…"

Phys. Rev. 120, 300 (1960).

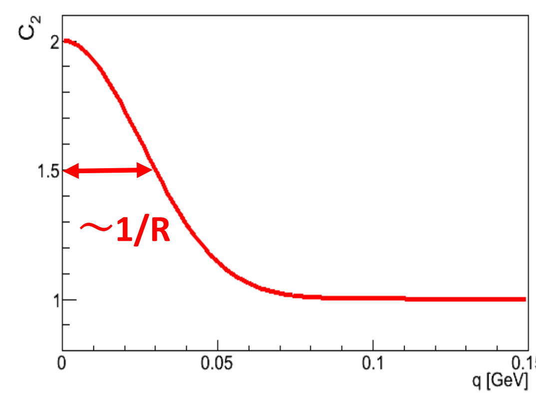

The development of HBT interferometry

In the1970s, these methods were refined and reconfirmed by Kopylov and Podgoretsky, Koonin, and Gyulassy, and other classes of correlations were shown. Some factors are useful for source-size measurements, such as strong and Coulomb interactions.

- Similar measurements for neutrons evaporated from highly excited nuclei → the shape of nuclei and their mean lives; for pions from the resonance decay → the mean resonance life.

- Correlations between protons emitted with nearly equal momenta are shown to be sensitive to the space-time structure of high-energy heavy-ion collisions.

- R can be used to determine the degree of coherence of the produced pion field as well as the geometric structure of the source of the chaotic field component.

- Final-state interactions, Coulomb interactions and the exclusion principle will influence the size, velocity, and lifetime of the collision volume.

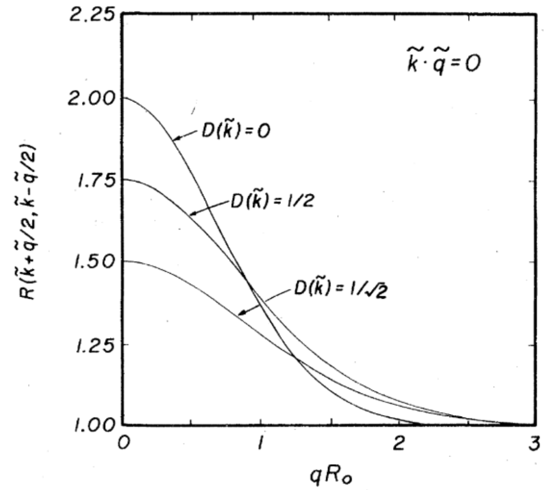

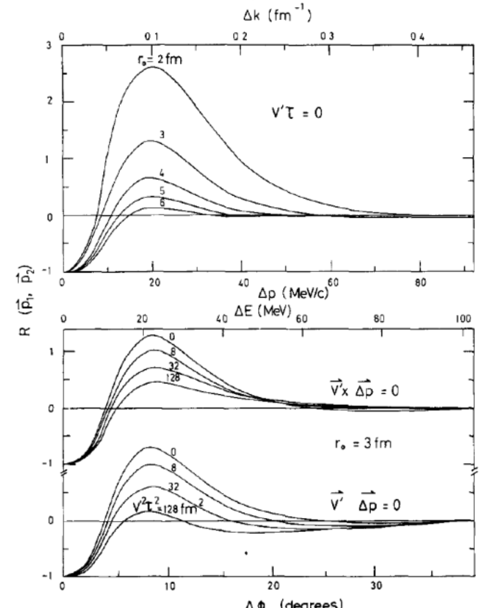

Phys. Lett. B 50,472 (1974). Sov. J. Nucl. Phys., 15,219(1972), 18,336 (1974).
Phys. Lett. B70:43 (1977). Phys. Rev. C 20, 2267(1979).

The applications in heavy ion collisions

- In 1986, the radii of the pion emission region obtained from interfermometry measurements in HICs, have been compiled and shown to be close to the effective nuclear radius of the lighter nucleus.

The experimental data were sufficient to demonstrate a crude scaling of the one-dimensional radii, indicating that spatial scales were indeed being probed

$$R_I = 1.21 A_p^{1/3}$$

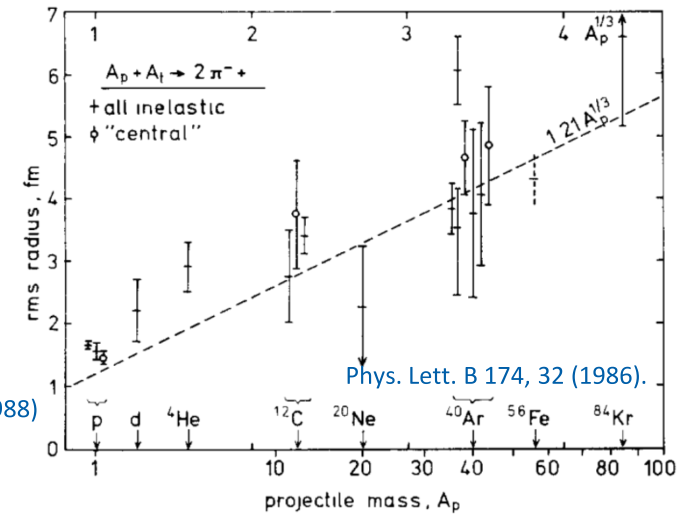

Phys. Lett. B 174, 32 (1986).

- The femtoscopic measurements for relativistic HICs were presented by the NA35 Collaboration (^{16}O+Au@200 GeV/nucleon). Z. Phys. C 38:79 (1988). Phys. Lett. B203:320 (1988)

AGS: E802 Coll. Si+Au@14.6A GeV/c. Phys. Rev. Lett. 69:1030 (1992)
SPS: NA44 Coll. S +Pb@200GeV/c. Phys. Lett. B 302, 510 (1993)
AGS: E814 Coll. Si+Pb@14.6A GeV/c. Phys. Lett. B 333, 33 (1994) .
…

-

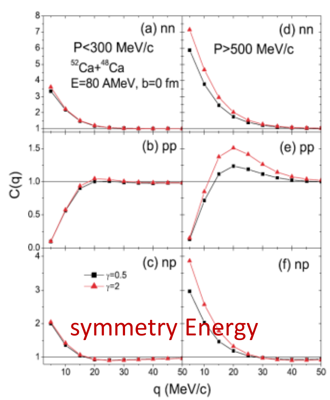

Phys Rev Lett. 90 162701 (2003)

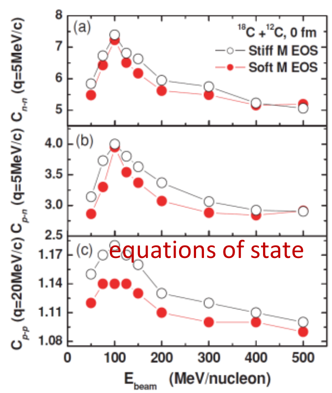

Phys. Rev. C 73, 014604 (2006)

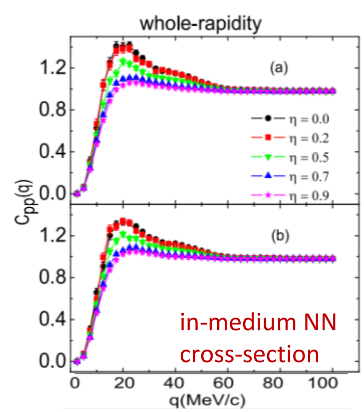

Phys. Rev. C 97, 034617 (2018)

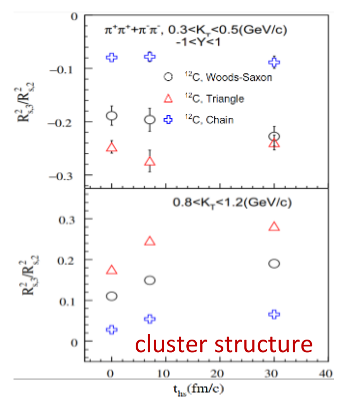

Eur. Phys. J. A 56, 52 (2020).

The applications in heavy ion collisions

- The EoS remains sufficiently soft in the transition region to delay the propagation of ordinary rarefaction waves for a considerable time. The signature of time delay, proposed by Pratt and Bertsch, is an enhancement of the ratio of the inverse width of the pion correlation function in out-direction to that in side-direction.

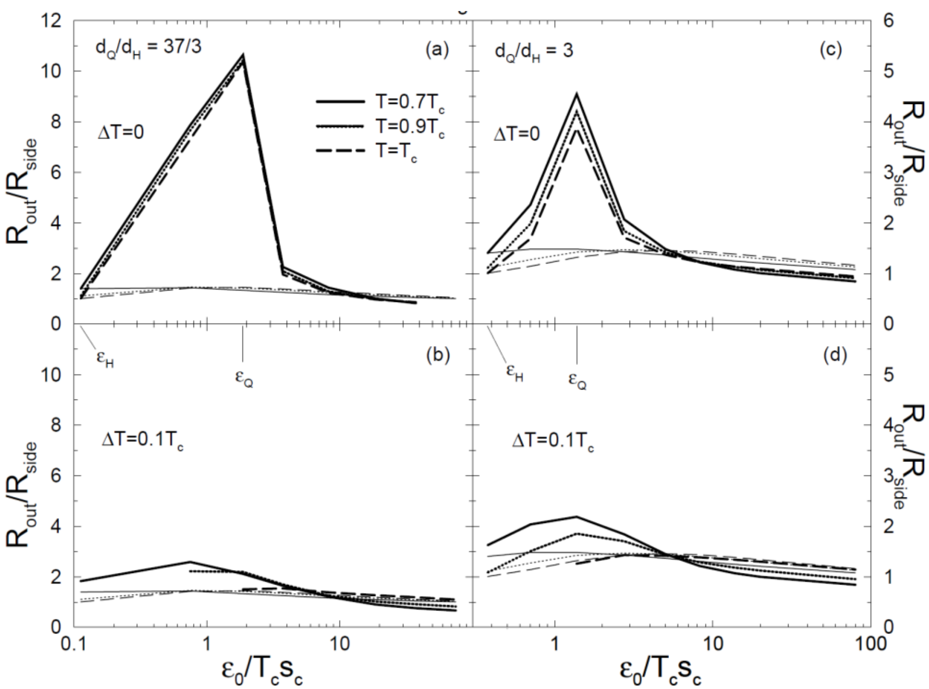

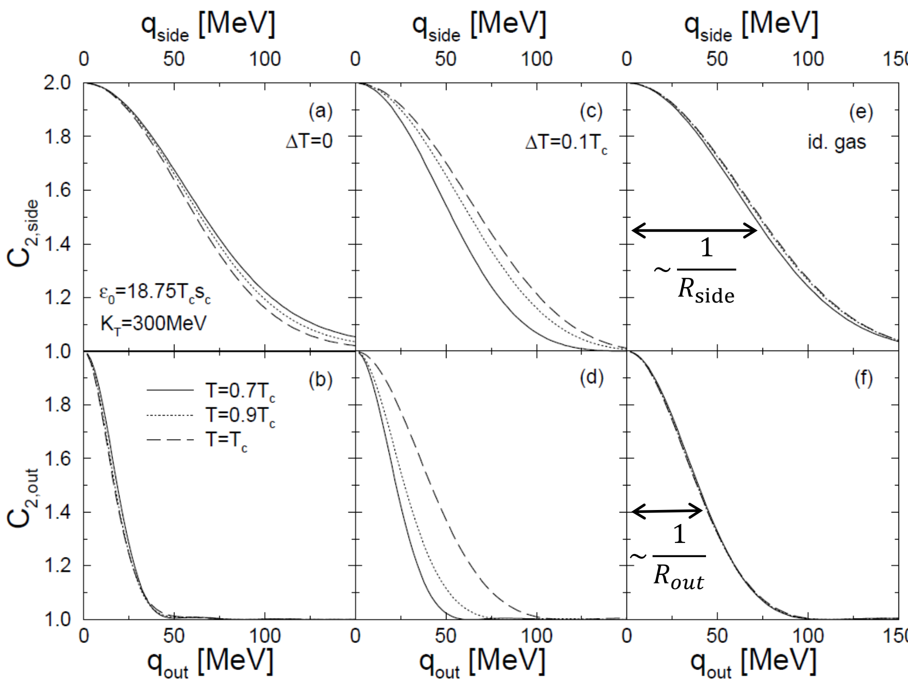

R_{out}, along the pair transverse momentum,
R_{side}, along the perpendicular direction in the transverse plane.

Phys. Rev. D 33, 1314 (1986). Phys. Rev. C.37.1896 (1988).
Nucl. Phys. A 608, 479 (1996). arXiv:nucl-th/9606039

HBT interferometry and QCD phase transition--experiment

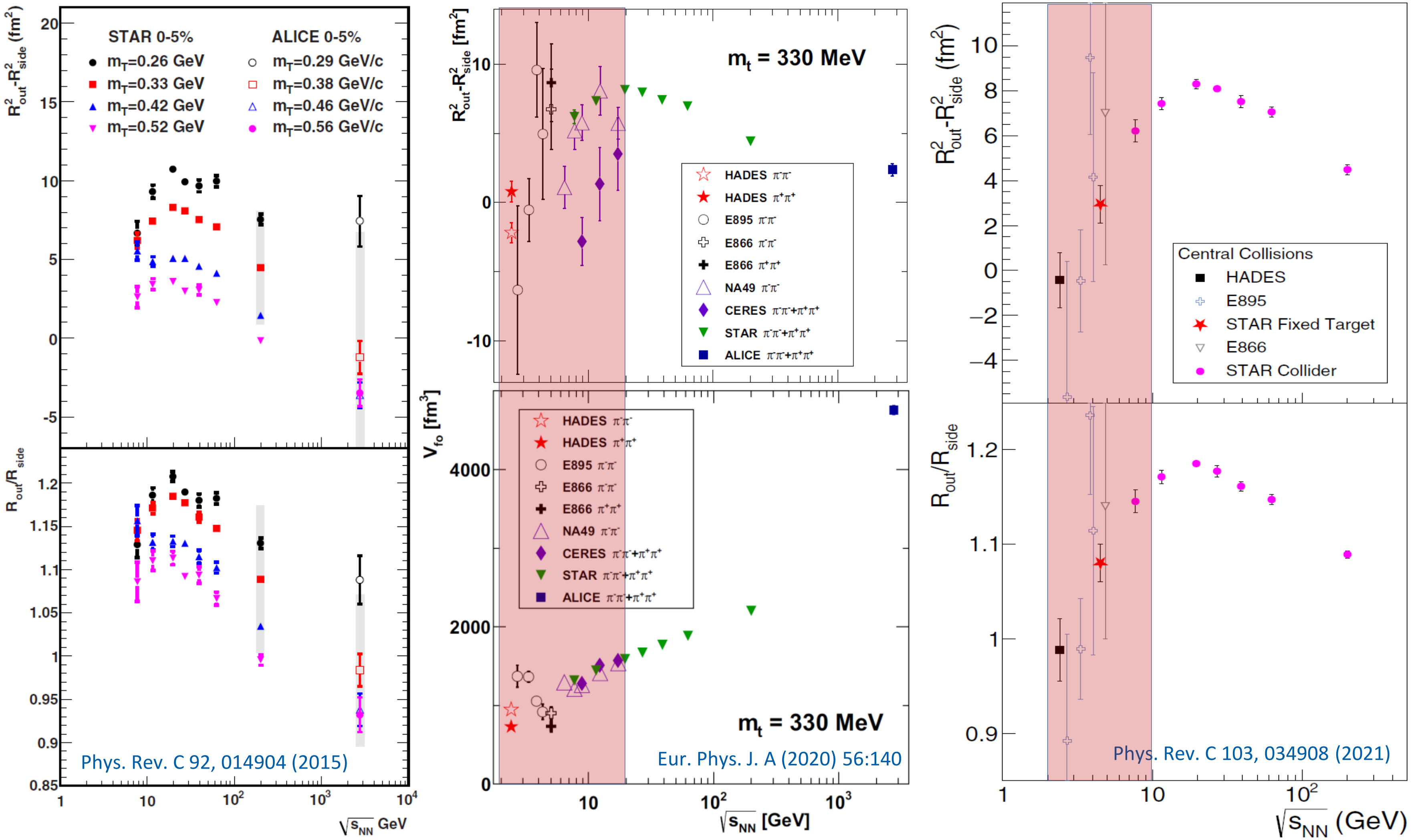

A wide maximum near $\sqrt{s_{NN}} \approx 20$ GeV.

In the most interesting energy region, the experimental data shows large uncertainties.

HBT interferometry and QCD phase transition—model calculations

AMPT: The effects of the hadronic mean-field potentials on the HBT correlation in relativistic HICs were studied.

The hadronic mean-field potentials are found to delay the emission time of the system and lead to large HBT radii extracted from the correlation function. (Soft attractive mean-field potentials at lower densities delay the emission of pions and baryons). C. J. Zhang, J. Xu, Phys. Rev. C 96, 044907 (2017)

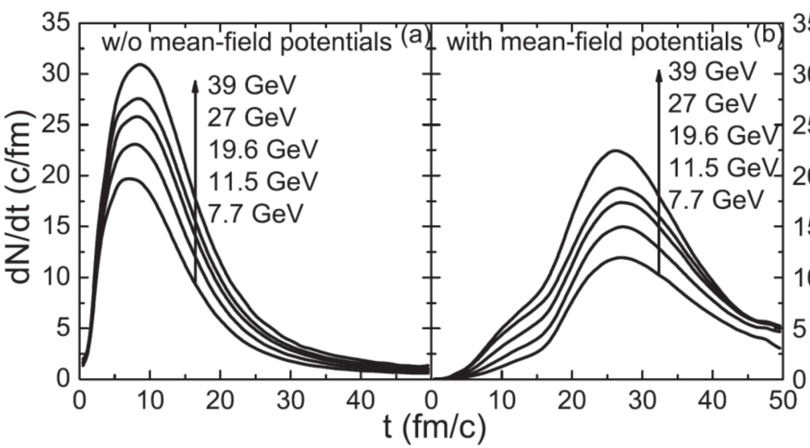

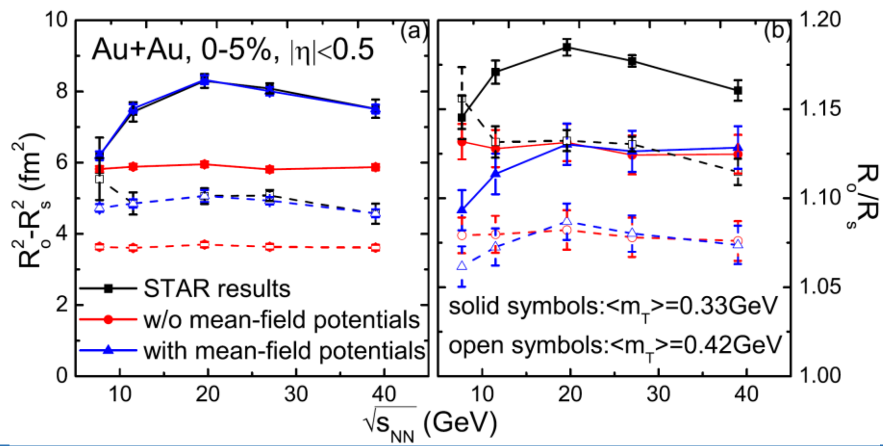

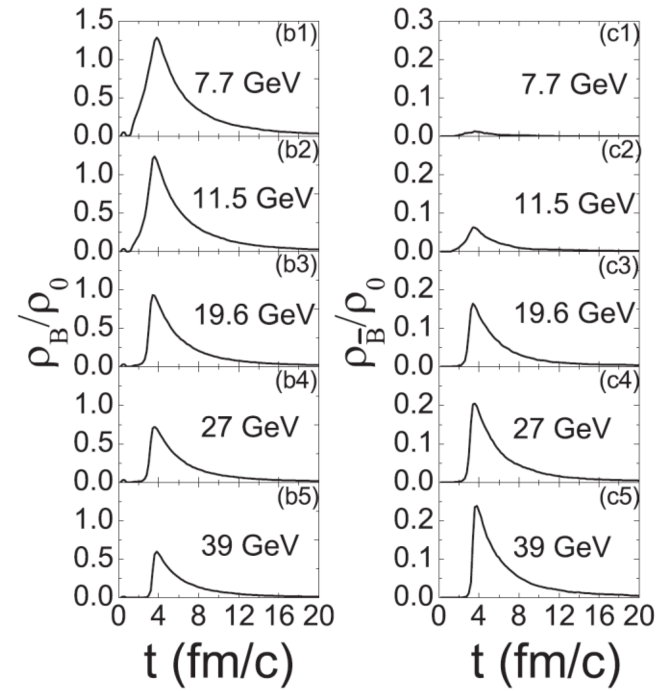

The HBT correlations can also be useful in understanding the mean-field potentials of protons, kaons, and antiprotons as well as baryon-antibaryon annihilations.

HBT interferometry and QCD phase transition—model calculations

vHLLE+UrQMD:

The bag model EoS (1PT EoS, first order phase transition) results in a systematically worse reproduction of the data, the chiral model EoS (XPT EoS, crossover transition) results in a quite reasonable reproduction of the STAR data. P. Batyuk et.al., Phys. Rev. C 96, 024911 (2017)

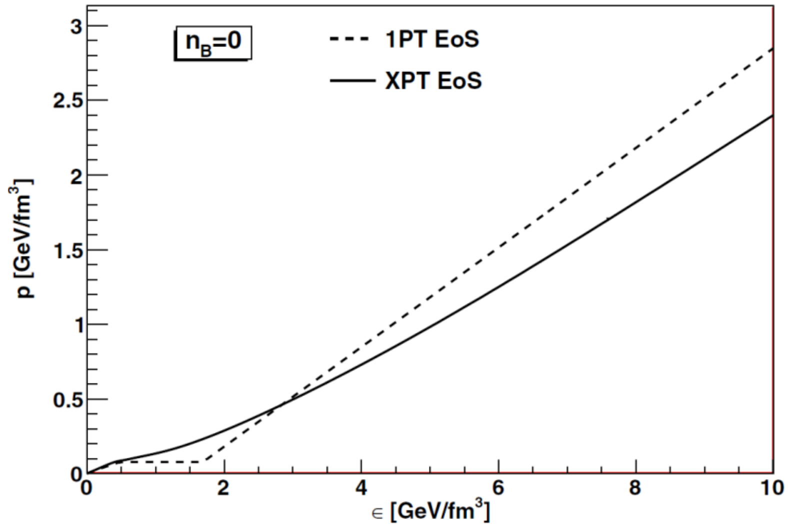

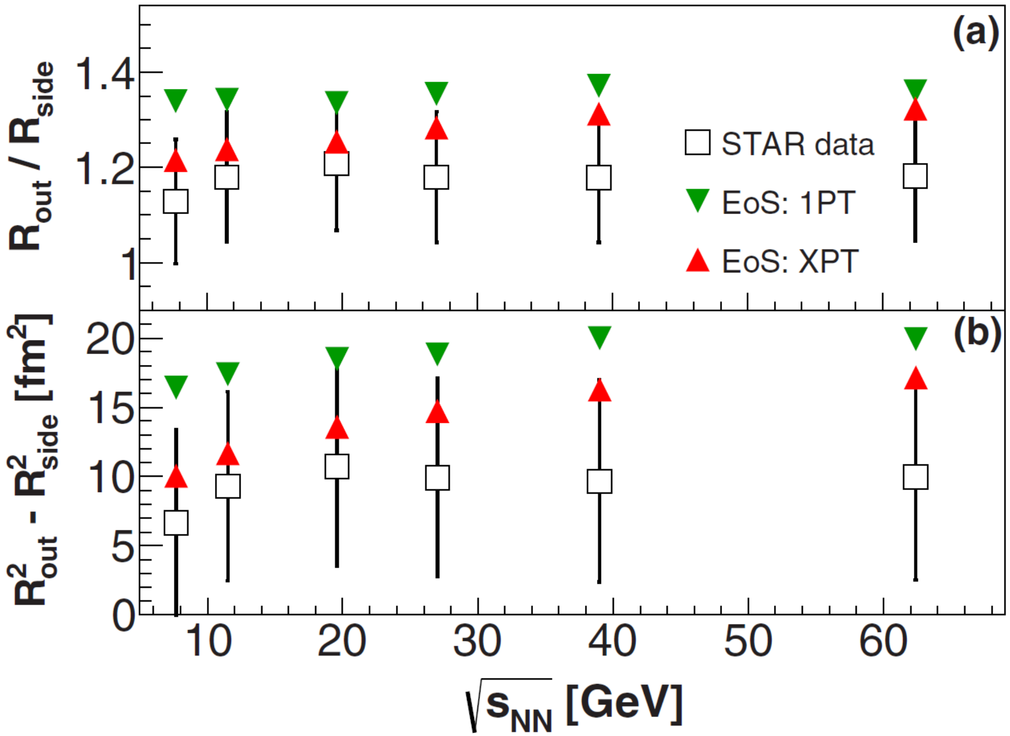

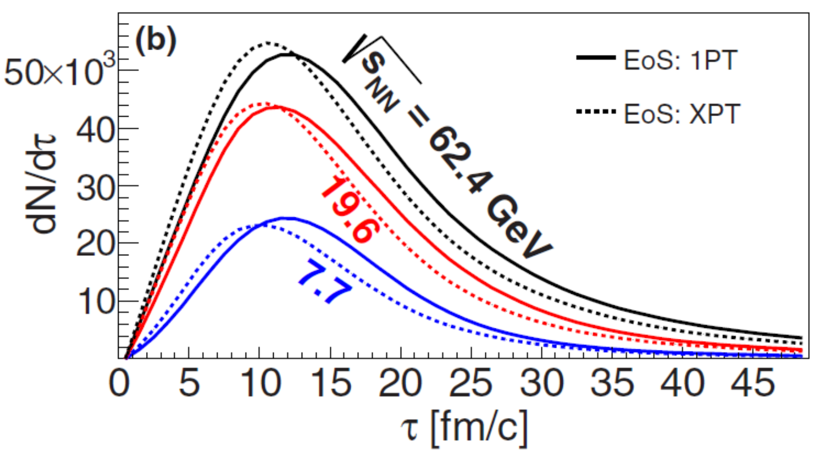

UrQMD calculations (previous)

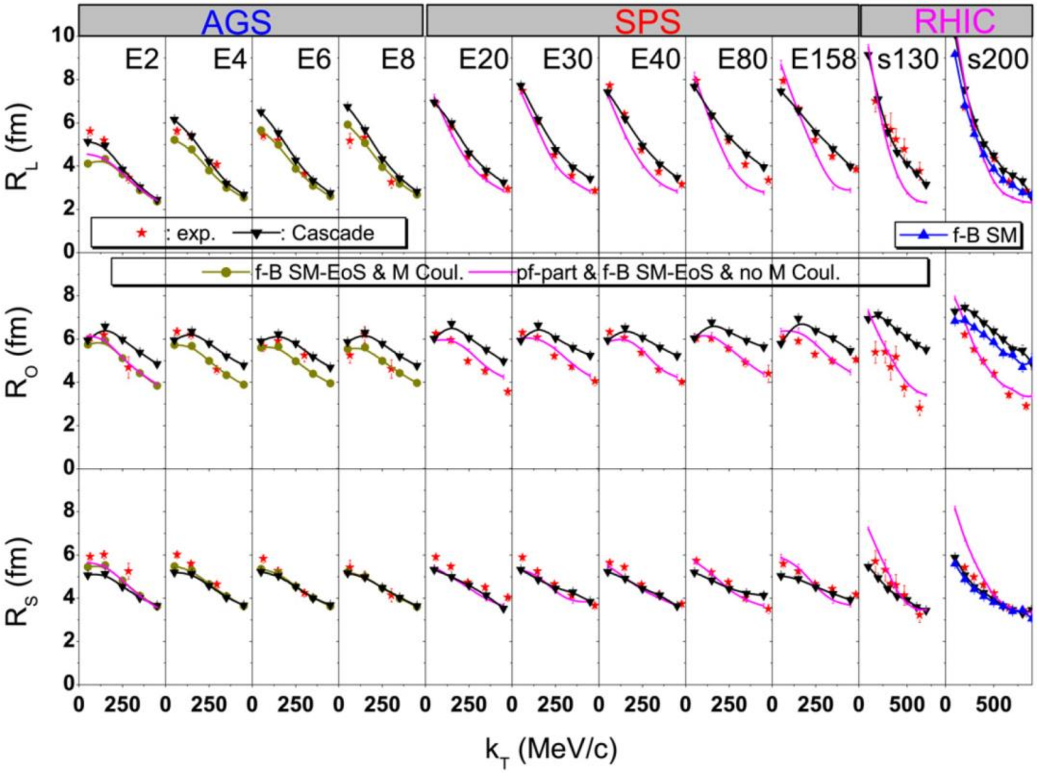

The mean field potentials for both confined and "pre-formed" particles (string fragments that will be projected onto hadron states later on) provides stronger pressure at the early stage.

The inclusion of potential interactions pushes down the calculated HBT radius R_O and pulls up the R_S so that the HBT time-related puzzle disappears throughout the energies from AGS, SPS, to RHIC.

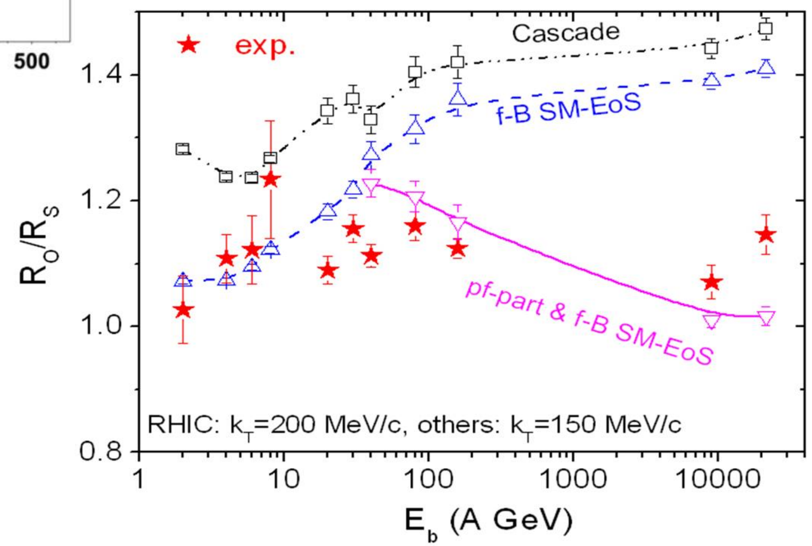

Q. Li et al. Phys. Lett. B 659 (2008) 525–530

UrQMD calculations (previous)

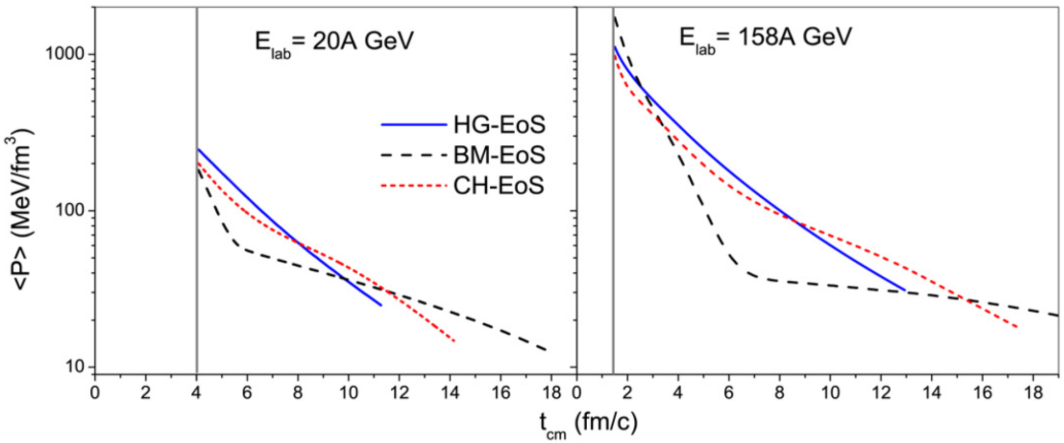

By incorporating a hydrodynamic stage into the UrQMD model, the effects of different equations of state and treatments of the hydrodynamic freeze-out procedure on the HBT radii were investigated.

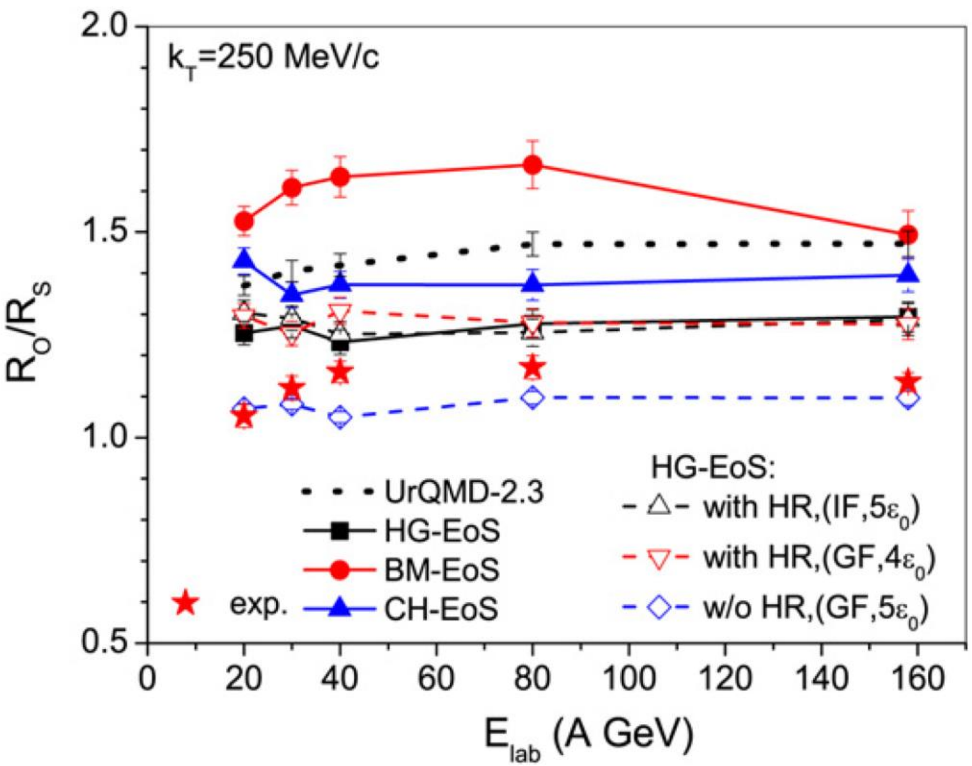

The HBT radii and the R_O/R_S ratio are sensitive to the EoS that is employed during the hydrodynamic evolution and the and treatments of the hydrodynamic freeze-out procedure.

Q. Li, et al., Phys. Lett. B 674 (2009) 111–116.

UrQMD model

The change of momentum of each baryon in accord with Hamiltons equations of motion can be calculated as

$$\dot{\mathbf{p}}_i = -\frac{\partial \mathbf{H}}{\partial \mathbf{r}_i} = -\frac{\partial \mathbf{V}}{\partial \mathbf{r}_i} = -\left(\frac{\partial V_i}{\partial n_i} \cdot \frac{\partial n_i}{\partial \mathbf{r}_i}\right) - \left(\sum_{j \neq i} \frac{\partial V_j}{\partial n_j} \cdot \frac{\partial n_j}{\partial \mathbf{r}_i}\right), \quad U(n_B) = \frac{\partial\left(n_B \cdot V(n_B)\right)}{\partial n_B} .$$

☐ The Skyrme model

The density dependence of the single particle potential for all baryons is given by a simple form:

$$U_{\text{Skyrme}}(n_B) = \alpha(n_B/n_0) + \beta(n_B/n_0)^{\gamma} .$$

Parameters	Hard EoS	Soft EoS
α [MeV]	-124	-356
β [MeV]	71	303
γ	2.00	1.17

☐ The CMF model

The single nucleon potential is given by the interactions with the chiral and repulsive mean fields. At $T = 0$, it can be calculated from the self energy of the nucleons as:

$$\text{U}_{\text{CMF}} = m_N^* - m_N^{\text{vac}} - \mu_N^* + \mu_N$$

$$V_{CMF} = E_{\text{field}}/A = E_{\text{CMF}}/A - E_{\text{FFG}}/A$$

A phase transition can be simply included by adding another minimum in the potential energy, to provide for another metastable state in the mean-field energy per baryon at large densities. Eur. Phys. J. C (2022) 82:427, Eur. Phys. J. C (2022) 82:911

See the talk by Jan on 28. Nov.

UrQMD model

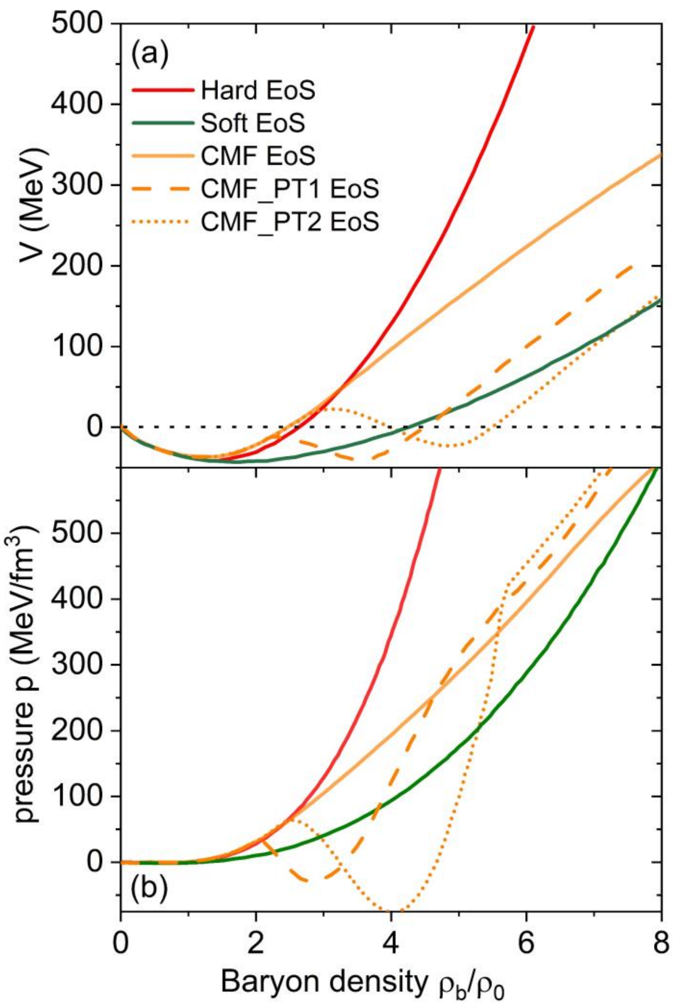

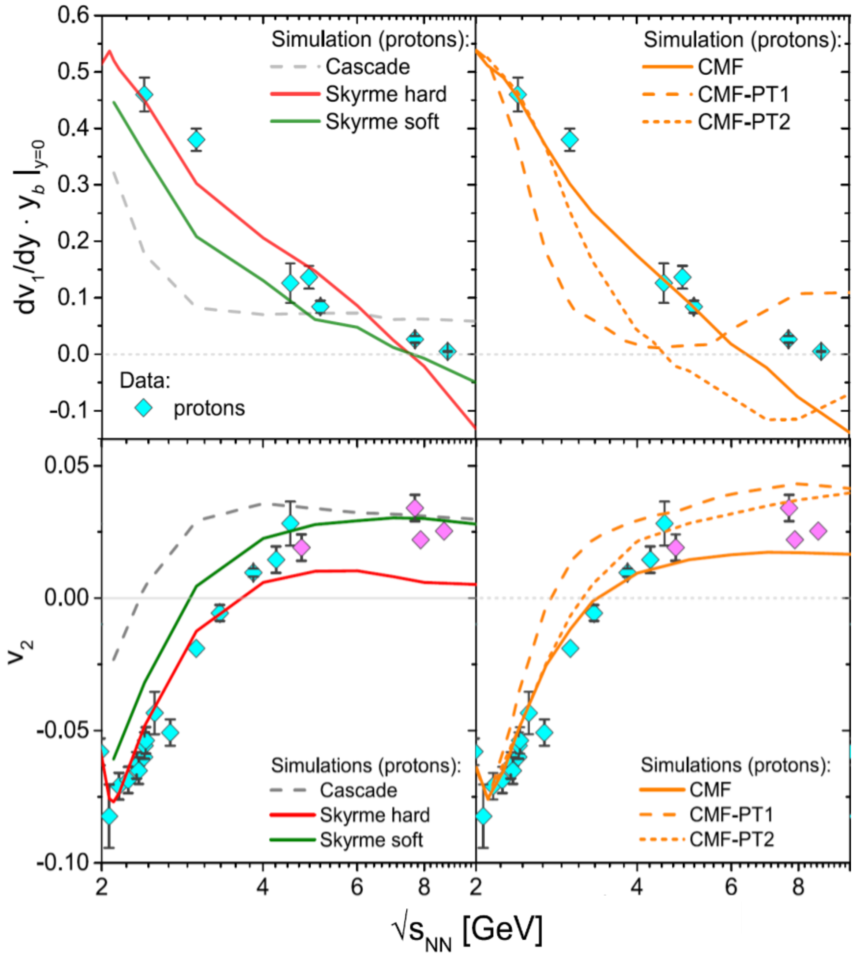

- The phase transitions with a low coexistence density ($\sim 4\rho_0$), shows a distinct minimum in the slope of the directed flow as a function of the beam energy.
- Excluding any strong phase transition at densities below$\sim 4\rho_0$.

J. Steinheimer et al., Eur. Phys. J. C (2022) 82:911

See the talk by Jan on 28. Nov.

UrQMD model

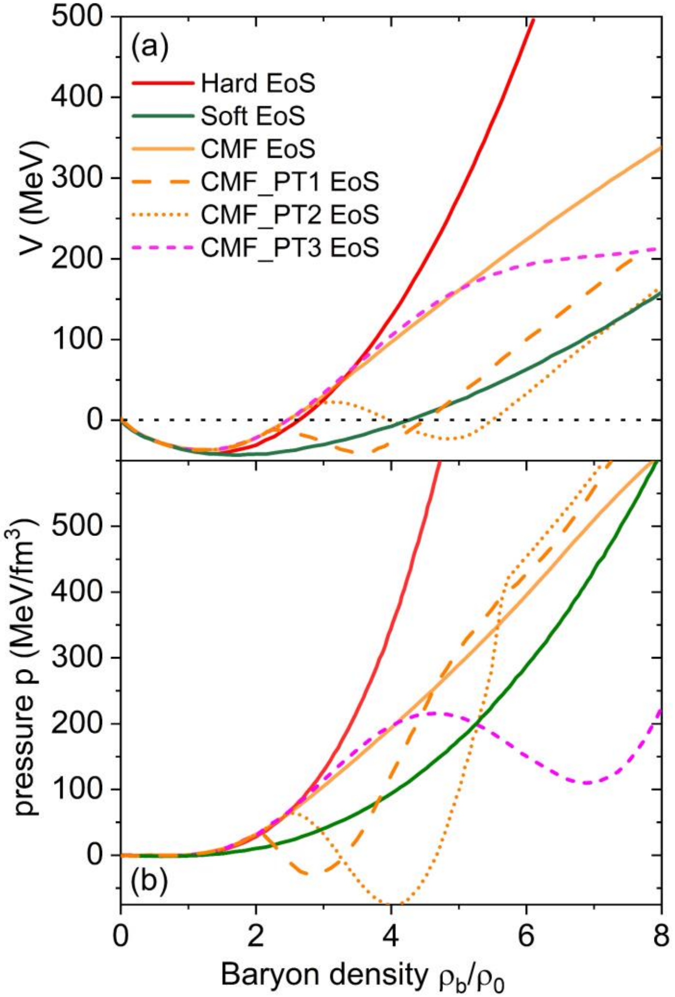

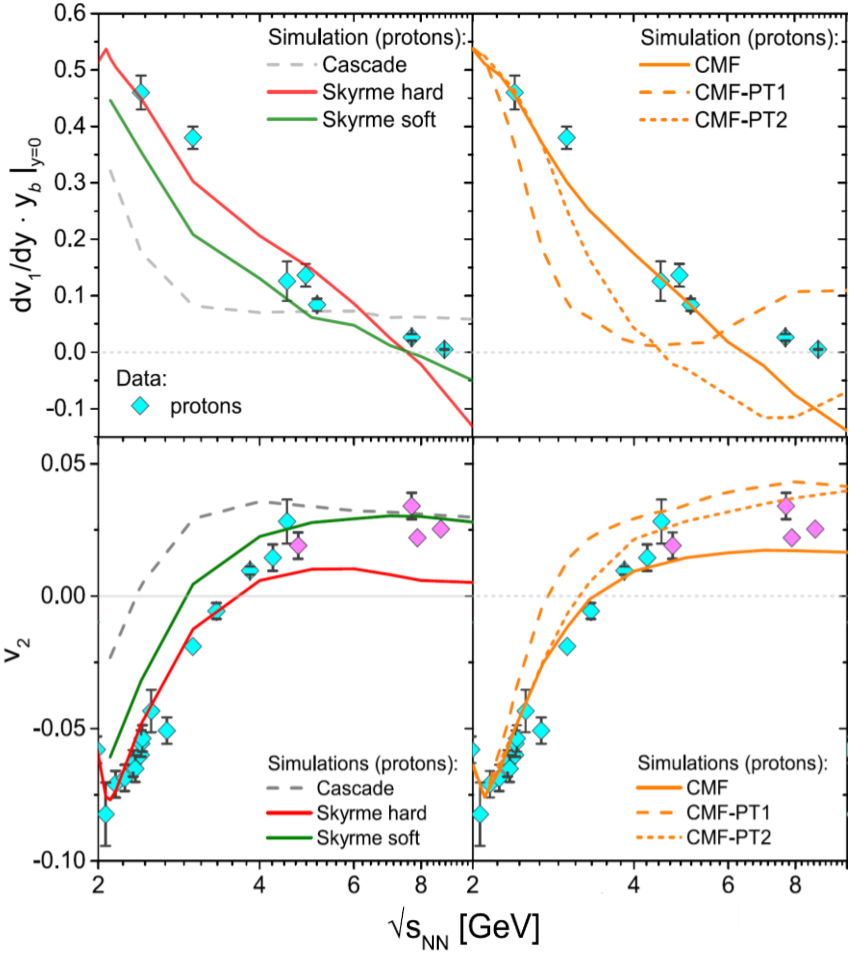

J. Steinheimer et al., Eur. Phys. J. C (2022) 82:911

See the talk by Jan on 28. Nov

- The phase transitions with a low coexistence density ($\sim 4\rho_0$), shows a distinct minimum in the slope of the directed flow as a function of the beam energy.
- Excluding any strong phase transition at densities below$\sim 4\rho_0$.

HBT interferometry

1. Performing UrQMD simulations, obtain the particles' freeze-out phase space coordinates.

2. The freeze-out space-time coordinates and 4-momenta serve as input for the "correlation afterburner" program (CRAB v3.0β) to construct the HBT correlator based on:

Phys. Rev. Lett. 53 (1984) 1219-1221.
https://web.pa.msu.edu/people/pratts/freecodes/crab/home.html

$$C(\mathbf{k},\mathbf{q}) = 1 + \frac{\int d^4x_1 d^4x_2 S_1(x_1,\mathbf{p}_1) S_2(x_2,\mathbf{p}_2) |\phi_{rel}(x_2' - x_1')|^2}{\int d^4x_1 d^4x_2 S_1(x_1,\mathbf{p}_1) S(x_2,\mathbf{p}_2)}$$

$S(x_i, p_i)$ is an effective probability for emitting a particle i with 4-momentum $p_i = (E_i, \mathbf{p}_i)$ from the space-time point $x_i = (\mathbf{r}_i, t_i)$.

ϕ_{rel} is the relative wave function in the pair's rest frame.

$\mathbf{q} = \mathbf{p}_i - \mathbf{p}_j$ and $\mathbf{k} = (\mathbf{p}_i + \mathbf{p}_j)/2$ are the relative momentum and the average momentum of the two particles i and j.

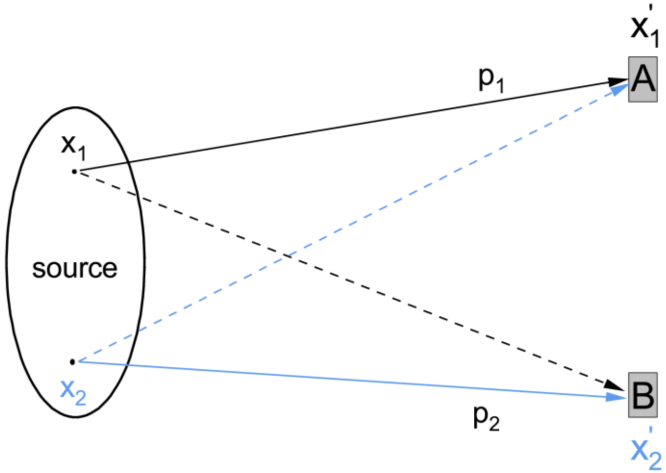

3. Lastly, the correlation function is then fitted assuming a 3D Gaussian form in the longitudinally comoving system.

Phys. Lett. B 270, 69 (1991). Phys. Lett. B 432, 248 (1998). Phys. Rev. C 103, 034908 (2021)

$$C(q_L, q_O, q_S) = N[(1-\lambda) + \lambda K_C(q_{inv}, R_{inv})(1 + e^{-R_L^2 q_L^2 - R_O^2 q_O^2 - R_S^2 q_S^2 - 2R_{OL}^2 q_O q_L})]$$

3D Bertsch-Pratt parametrization

$$C(q_L, q_O, q_S) = N[1 - \lambda + \lambda K_C(q_{inv})(1 + e^{-R_L^2 q_L^2 - R_O^2 q_O^2 - R_S^2 q_S^2 - 2R_{OL}^2 q_O q_L})].$$

The relative pair momentum, $\vec{q}$, is projected onto the Bertsch-Pratt coordinate system

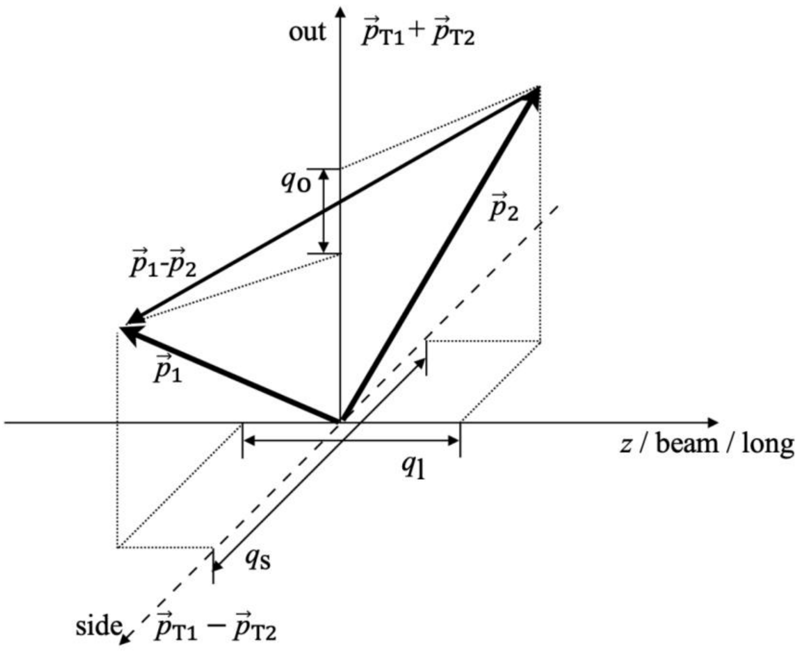

q_{long}: is parallel to the beam direction.
q_{out} : is parallel to the mean transverse momentum of the pair (k_T).
q_{side}: is perpendicular to the other two directions.

R_{long}: Longtudinal size
R_{side}: Transverse size
R_{out} : Transverse size + duration of particle emission

N: is the overall normalization factor,
λ : is the incoherence factor and lies between 0 (complete coherence) and 1 (complete incoherence) for bosons in realistic HICs.
R_{ol}^2: represents the cross-term and plays a role at large rapidity.

Coulomb interaction (FSI)

Bowler-Sinyukov method

The quantity K_C is the squared Coulomb wave function integrated over the entire spherical Gaussian source.

HBT correlation function

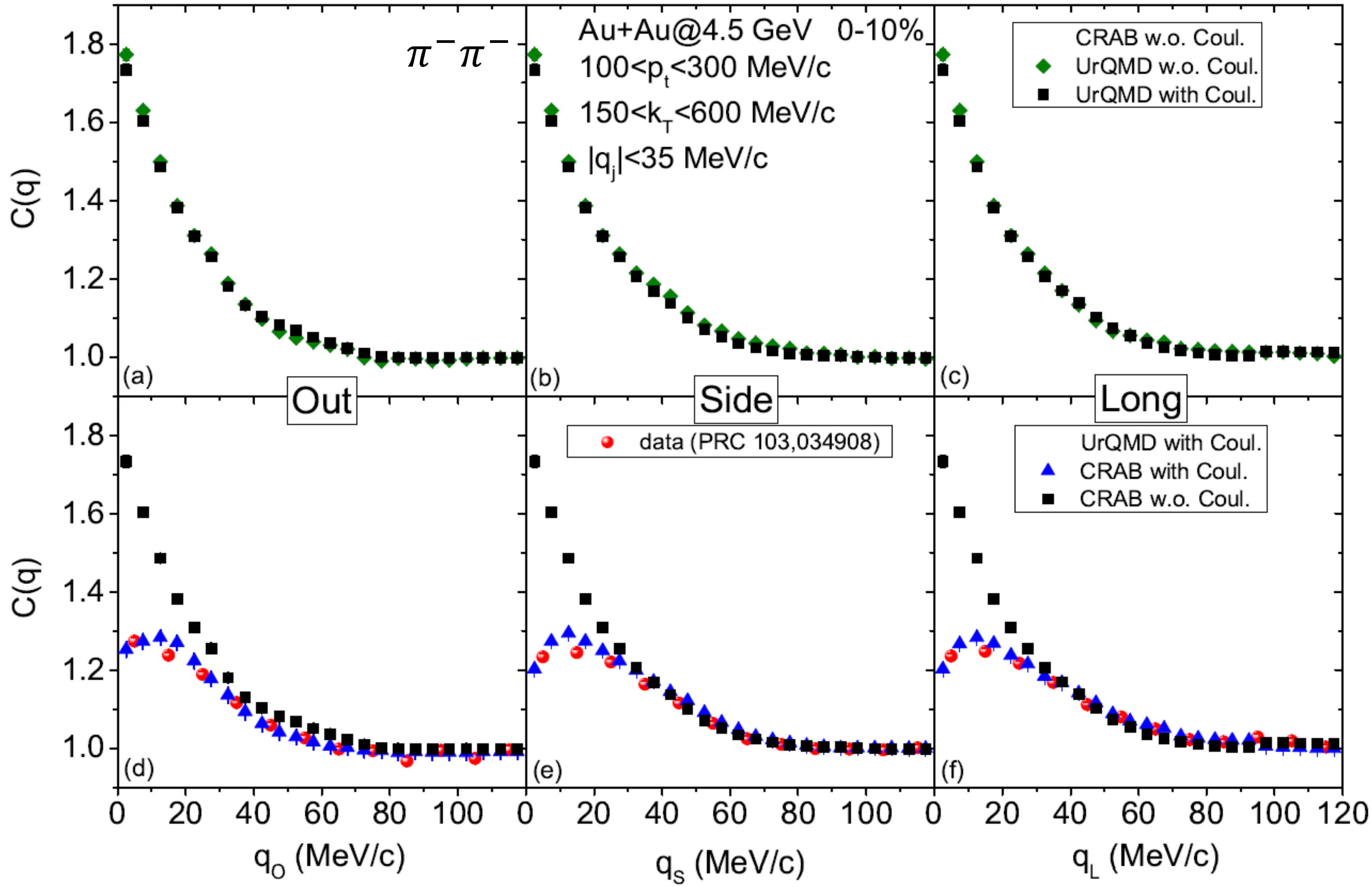

Coulomb effects before freeze-out on the correlation functions are weak, while Coulomb interactions in FSI have strong effects.

HBT correlation function

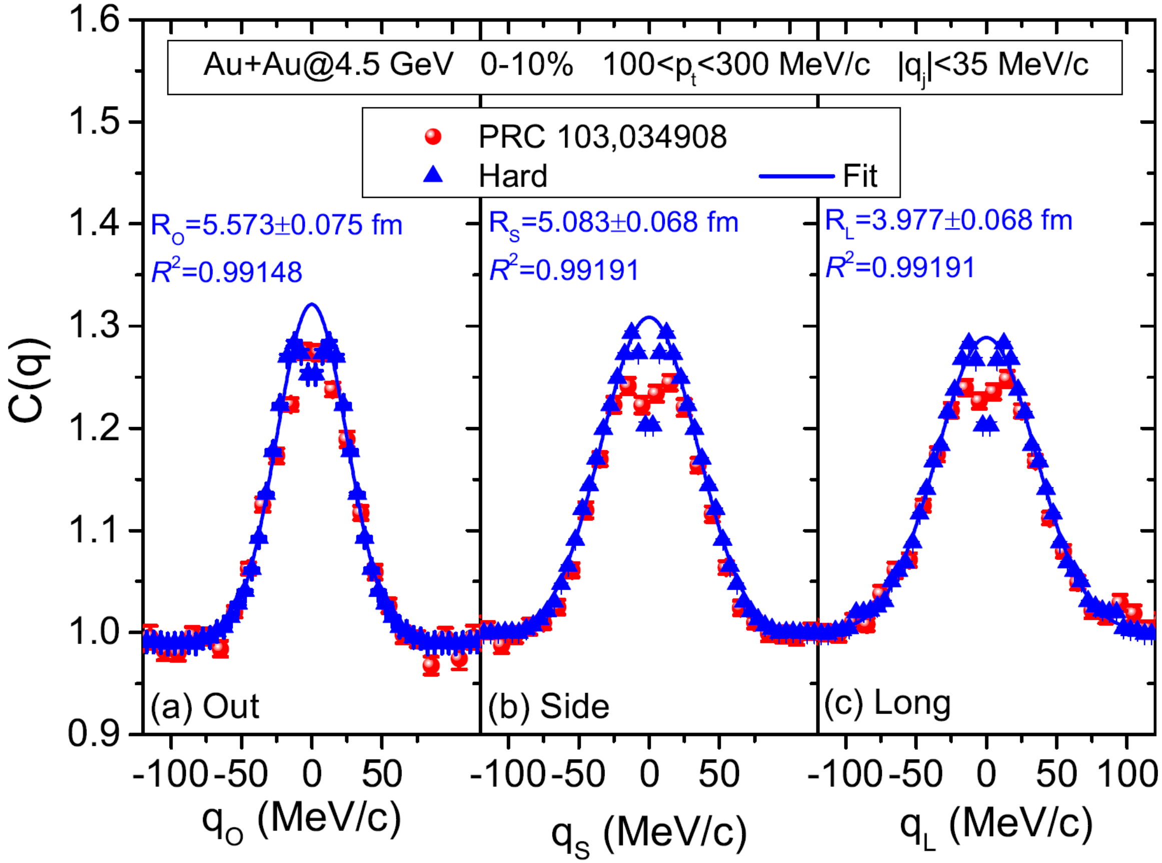

$$C(q_i) = N[(1-\lambda) + \lambda K_C(1+\exp(-R_i^2 q_i^2))]$$

The calculated $\pi^-\pi^-$ correlation functions can be reasonably reproduced by the one-dimensional Gaussian fitting. Thus, these reasonable fits can be used to extract radii that characterize the space-time extent of the source.

Mesonic Coulomb potential

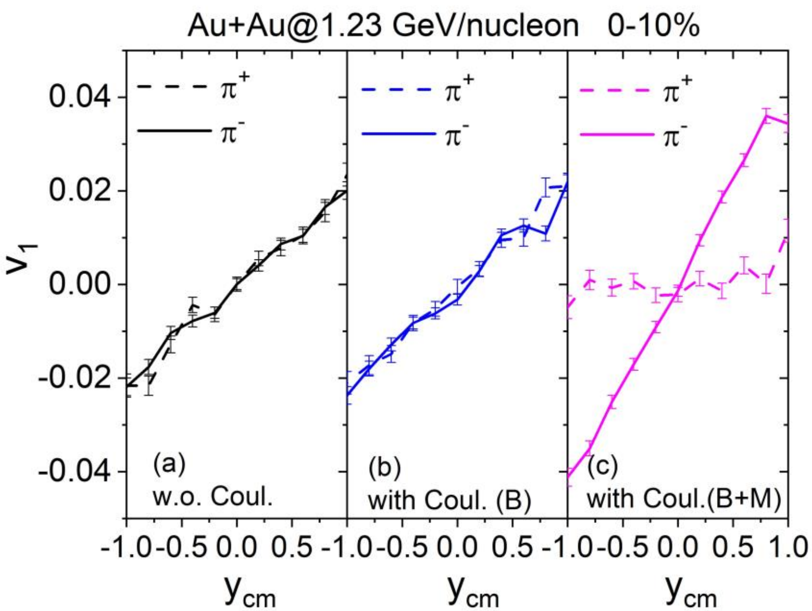

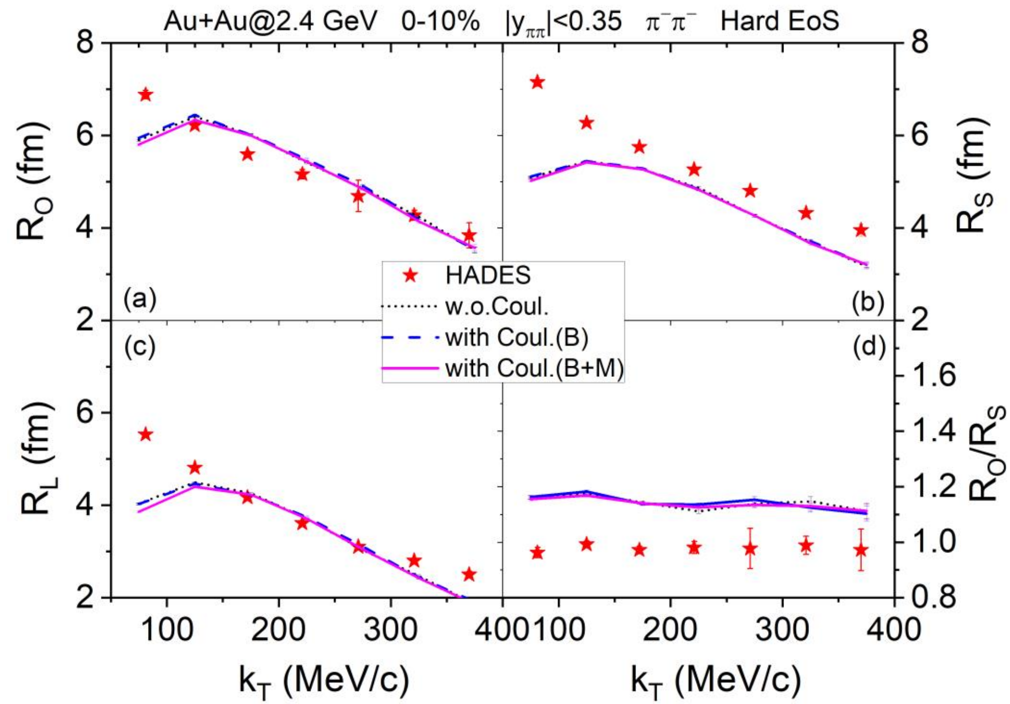

- The effects of the two-body mesonic Coulomb potential during the evolution on the HBT radii and the ratio R_O/R_S are very weak.

- Flows reflects the integrated collective motion of single particles;
  The size of the freeze-out source: two-pion correlation function in relative momentum.

EoS without phase transitions

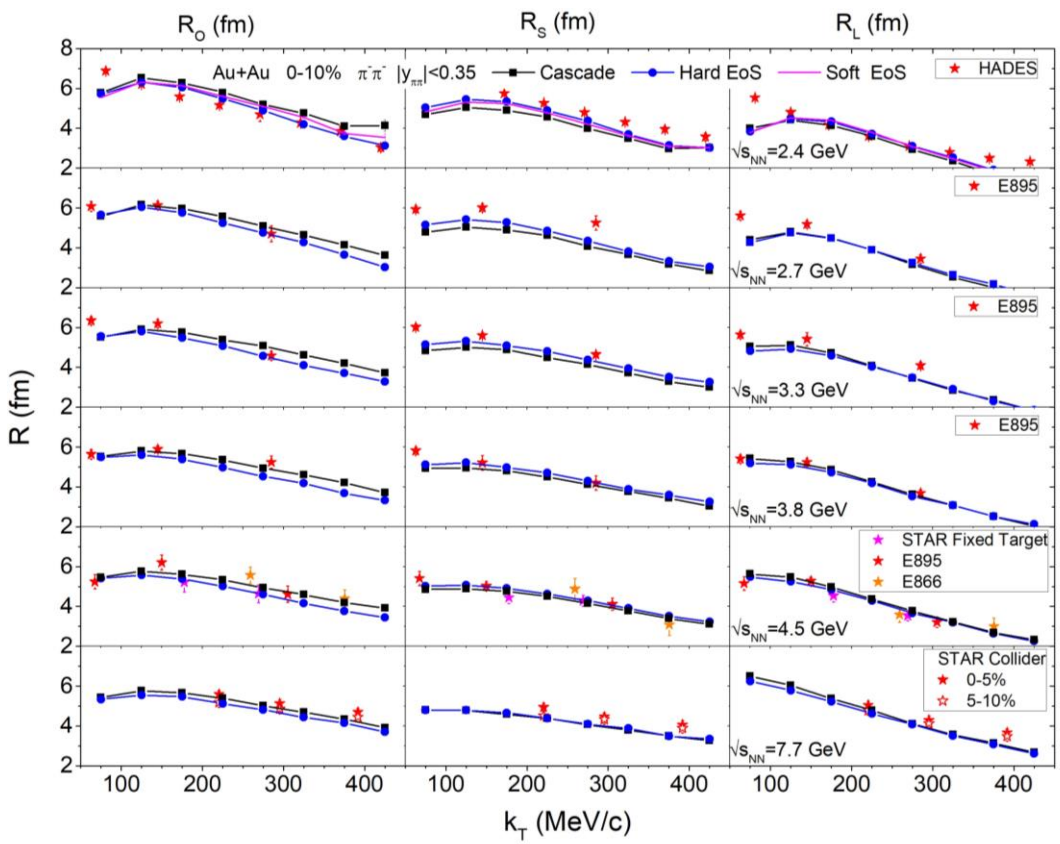

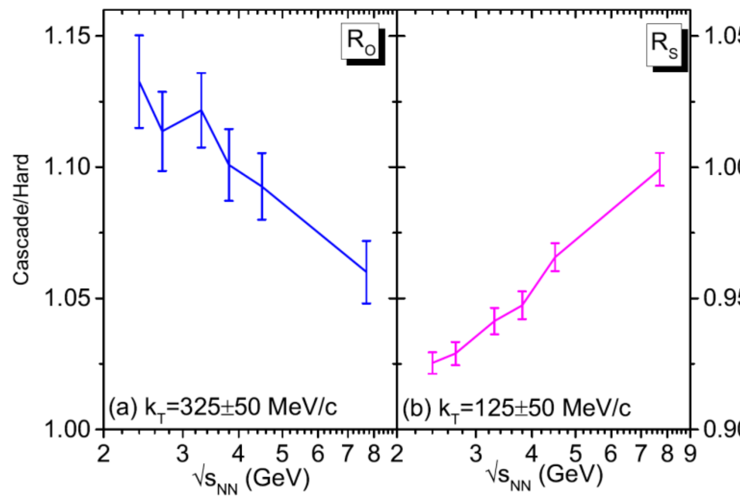

- Both the values of the HBT-radii and their decrease with k_T can be well reproduced by the calculations with a hard Skyrme potential EoS.
- With increasing stiffness of the potential (stronger repulsion as function of density), the R_O at large k_T is driven down while the R_S at small k_T is pulled up.

EoS with phase transitions

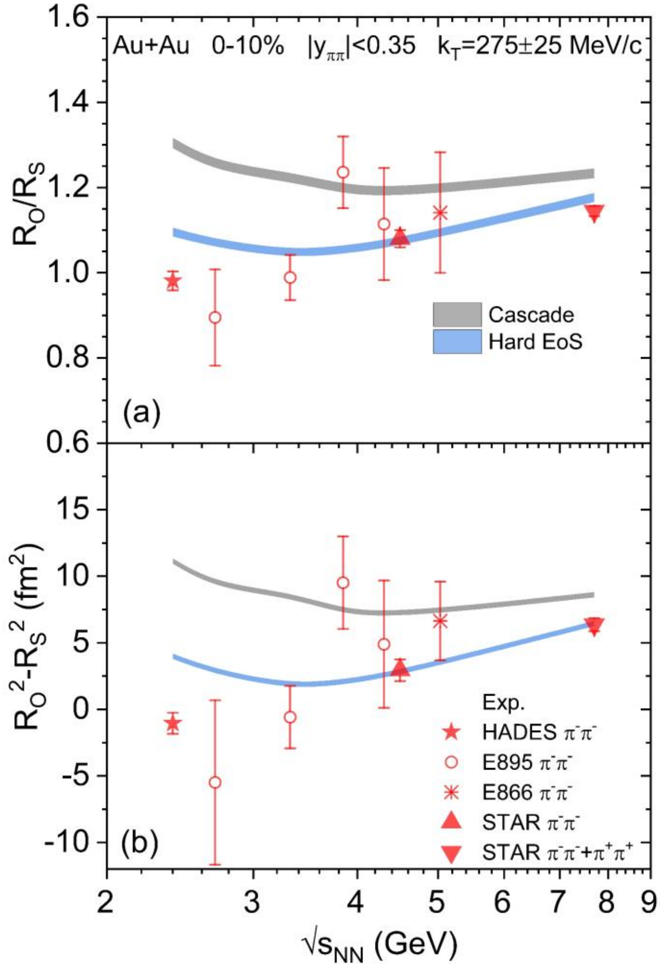

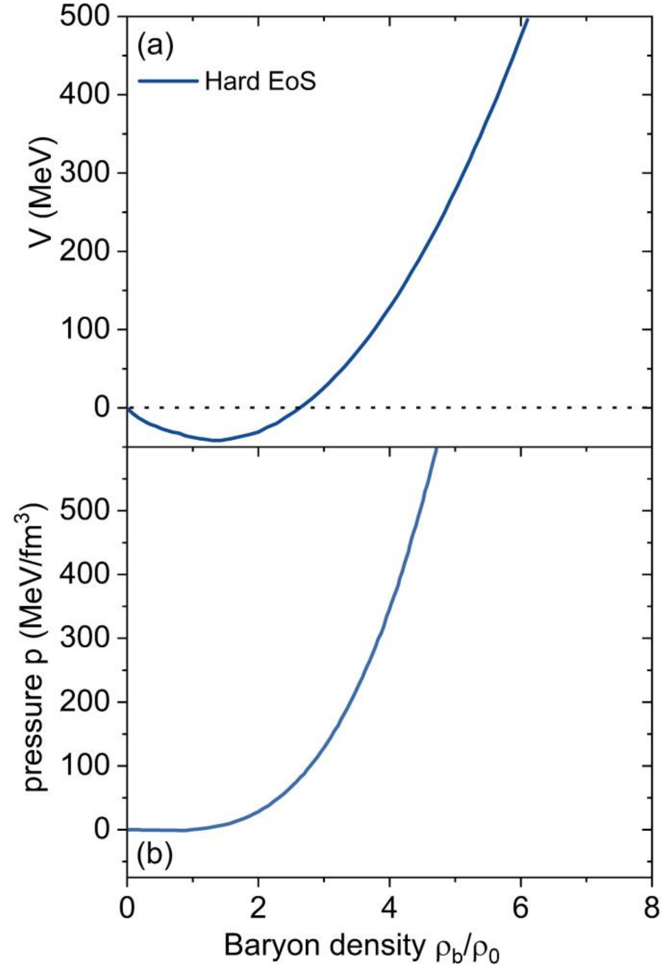

- A repulsive density dependent EoS will lead to a stronger phase-space correlation explaining the HBT time-related tensions.
- The effects of the density dependent equation of state on the HBT radii decreases with increasing collision energy.

EoS with phase transitions

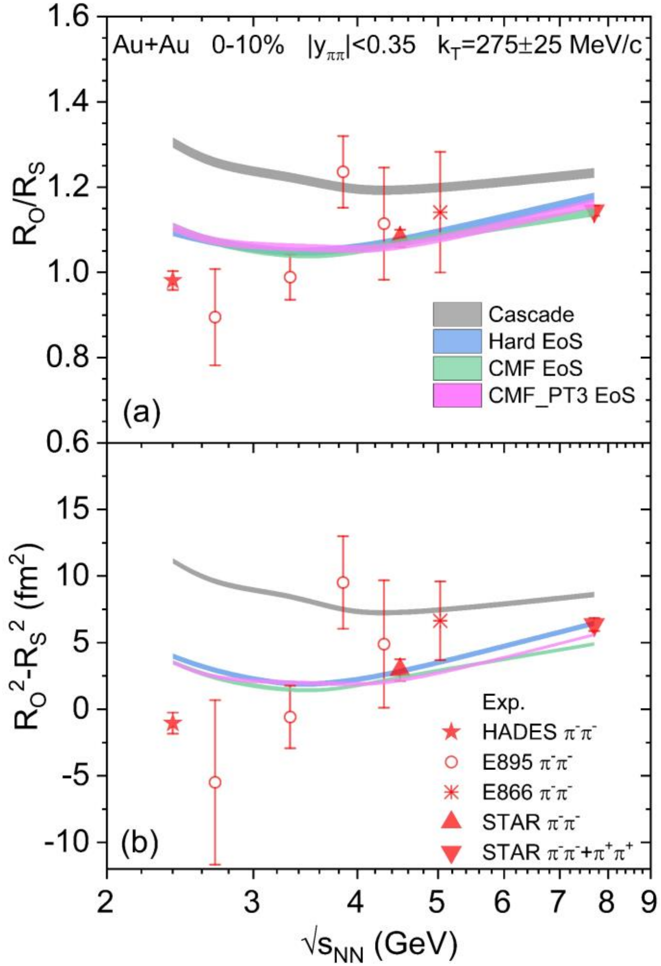

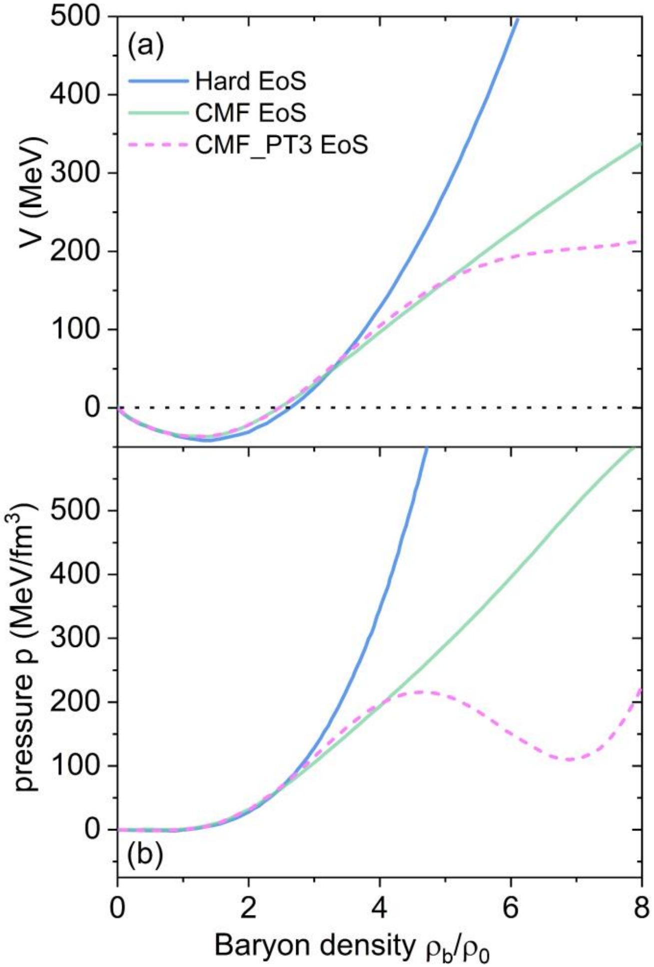

- In the investigated energy range, the CMF/PT3 EoSs give very similar results to the hard EoS which also includes a strong repulsion leading to earlier pion emission.
- The phase transition in PT3 is never really reached.

EoS with phase transitions

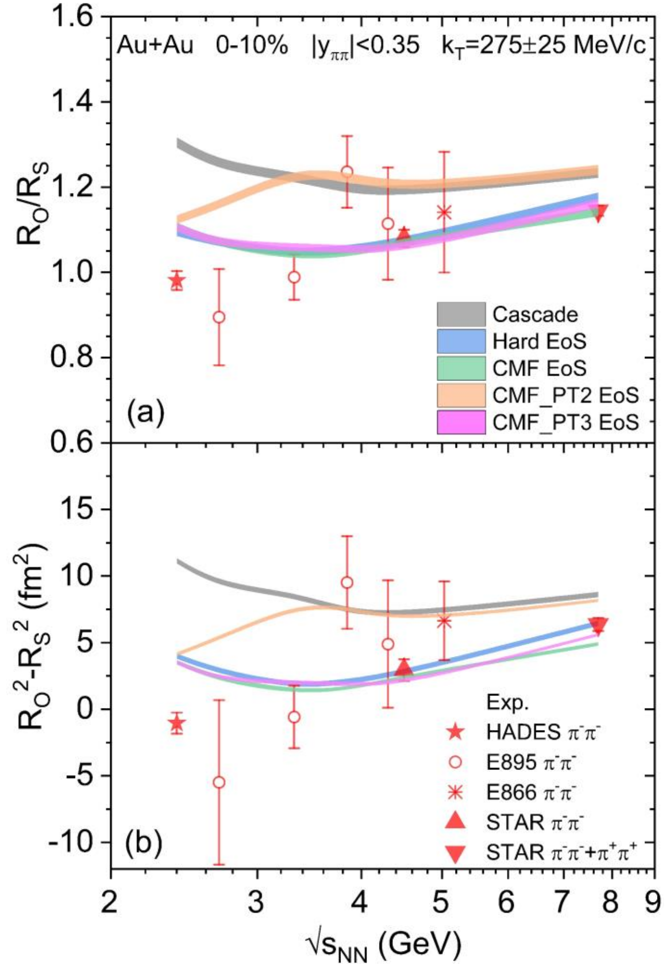

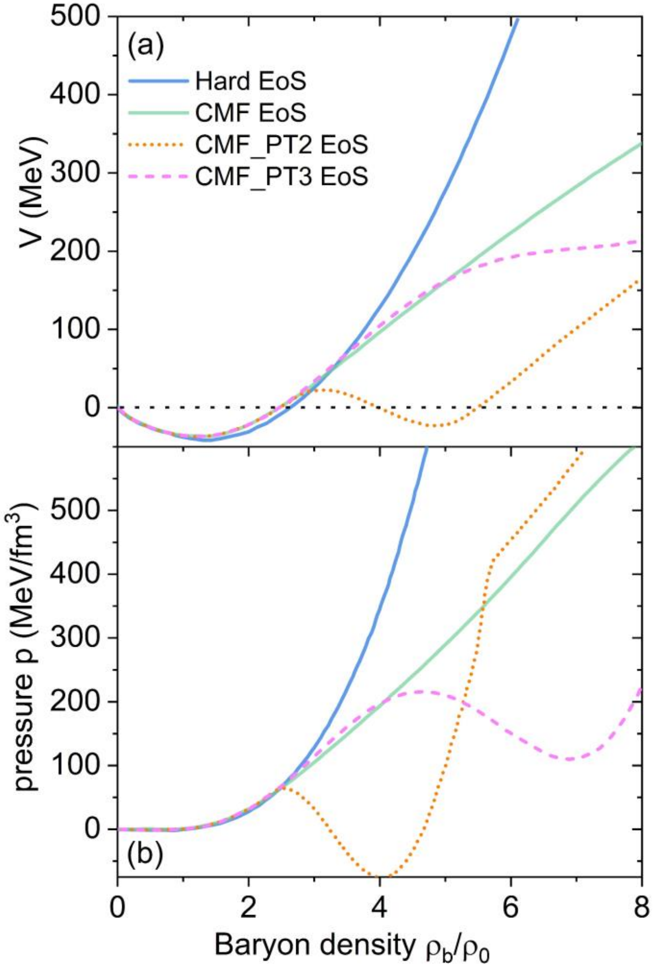

- As the collision energy increases, the calculated results of CMF PT2 EoS gradually increase compared to the standard CMF (or Hard/PT3) EoS as expected for the appearance of a phase transition.

Pion freeze-out time

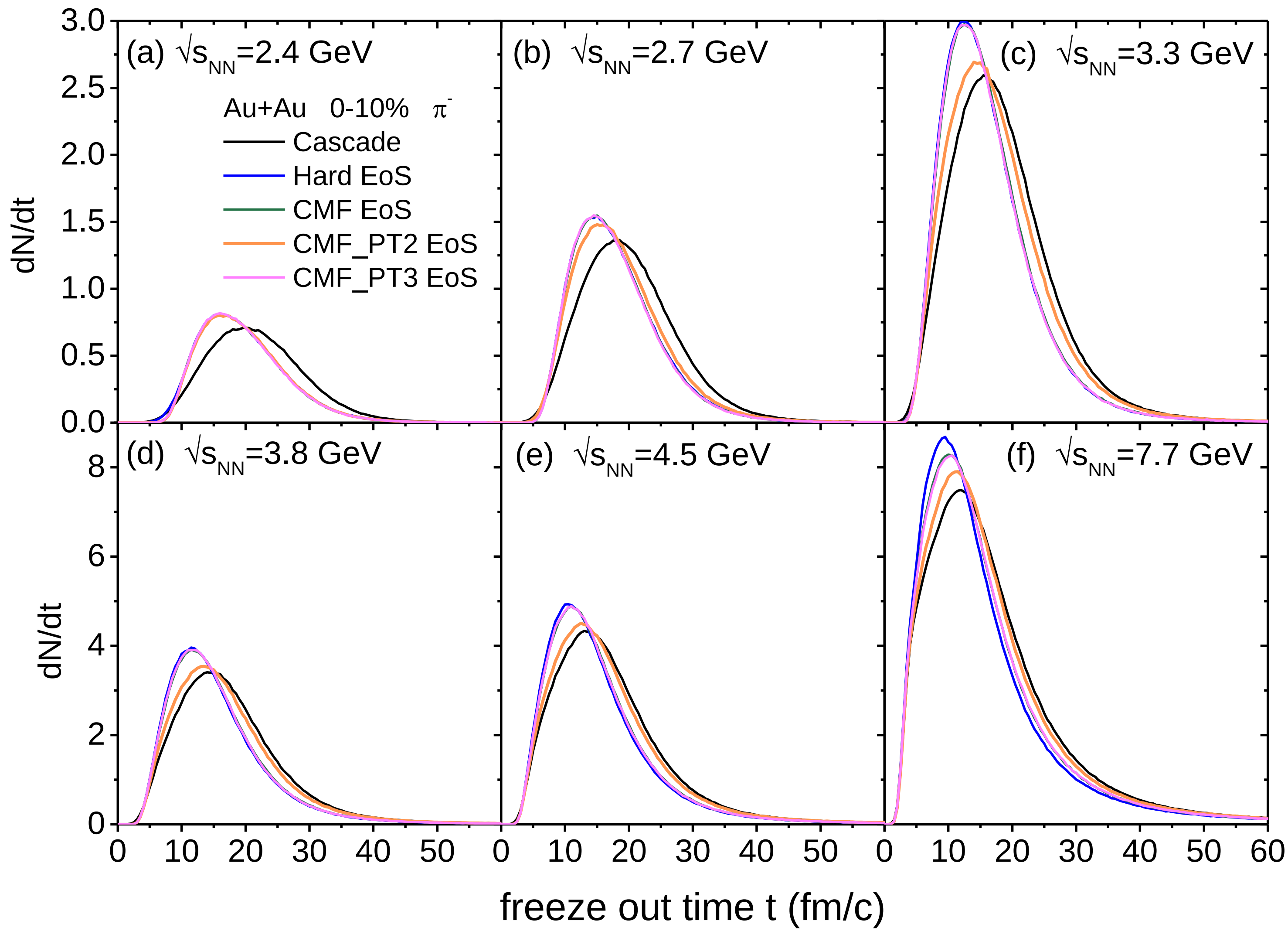

π^- are mainly frozen-out in the time interval 5-30 fm/c.

π^- are frozen-out earlier in case of a harder EoS.

Pion freeze-out time and coordinate distributions

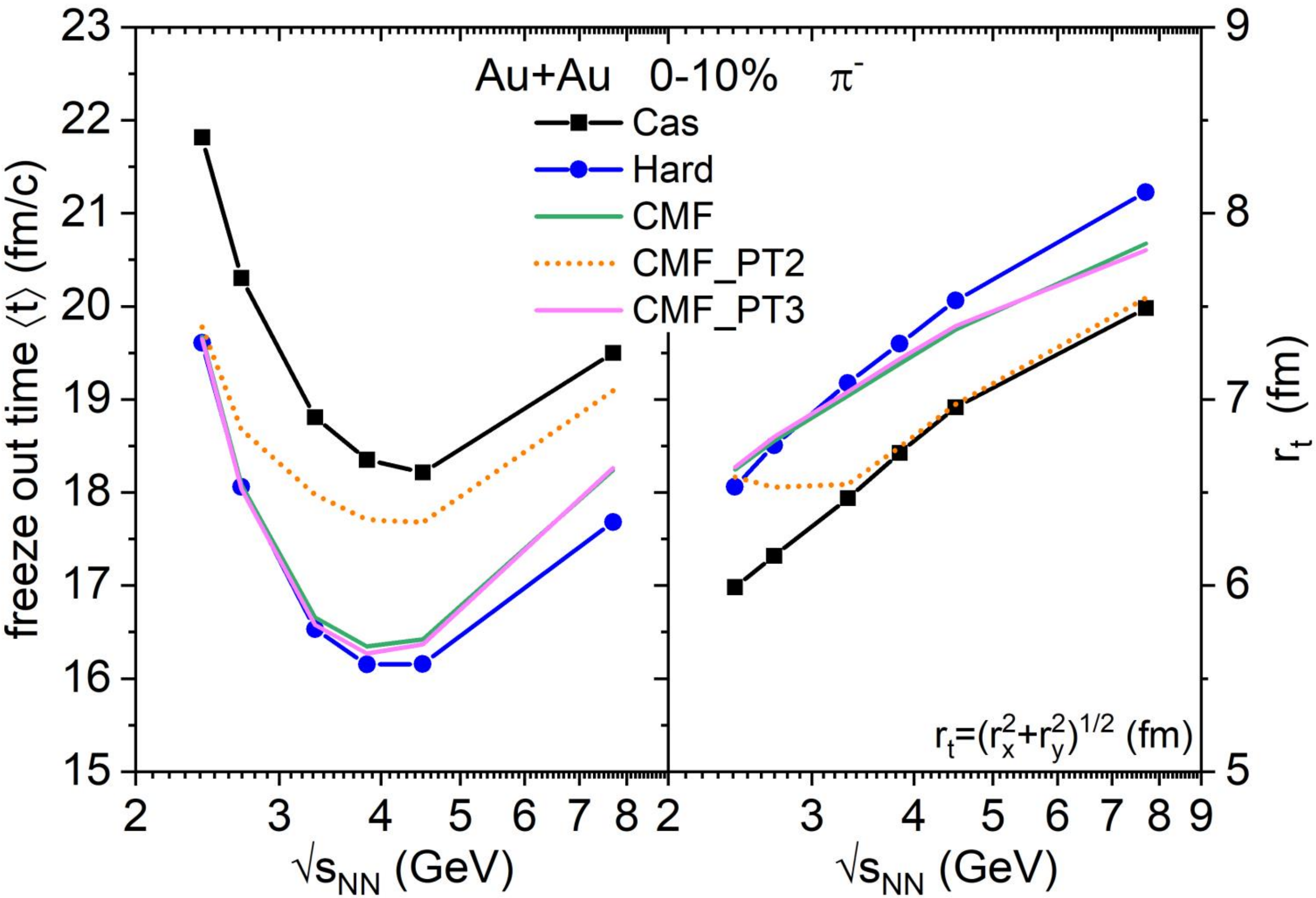

- The mean values of the freeze-out time (transverse radii) from hard EoS are smaller (larger) than that of the softer ones.
- The larger pressure generated by the potentials, leading to a stronger expansion, consequently larger transverse radii and an earlier freeze-out time.

Summary & Outlook

- The HBT radii and R_O/R_S are weakly affected by the Coulomb potentials during the evolution of the system.

- The source radii parameters (R_O/R_S and $R^2_O - R^2_S$) where shown to be sensitive to the EoS at densities up to $4{\sim}5\rho_0$.

- The present data, in the investigated energy region, can be qualitatively and quantitatively reproduced by simulations with an equation of state that shows stiff behavior up to $\sim 4\rho_0$ and a consecutive softening.

- By comparing to the available HBT data we can exclude the existence of a strong phase transition for densities up to $\sim 4\rho_0$.

- The effects of the density dependent EoS on the HBT radii are shown to decrease with increasing collision energy so that statements for higher densities are yet unreliable.

- More theoretical works on understanding the uncertainty from the model are needed.
- Highly accurate experimental data is desired.

Thank you for your attentions!

Back up

A simple example of HBT interferometry

The wave function for the two particles is:

$$A(k_1,k_2) = \frac{1}{\sqrt{2}}[e^{-ik_1.(x_A-x_1)}e^{i\phi_1}e^{-ik_2.(x_B-x_2)}e^{i\phi_2} \pm e^{-ik_1.(x_A-x_2)}e^{i\phi'_2}e^{-ik_2.(x_B-x_1)}e^{i\phi'_1}]$$

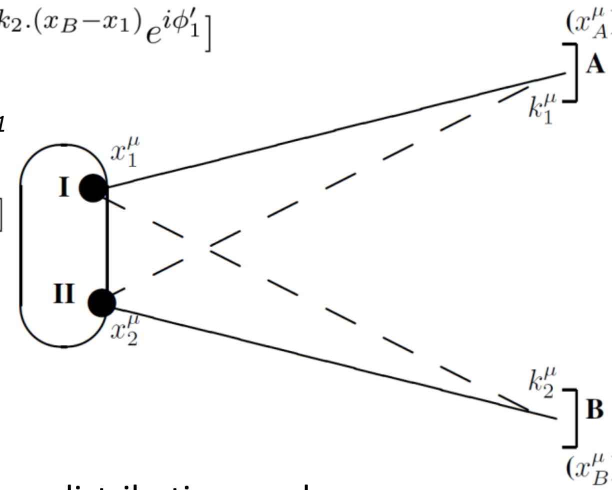

The probability for a joint observation of the two quanta with momenta k_1 and k_2 is given by

$$\begin{aligned} P_2(k_1,k_2) &= \langle |A(k_1,k_2)|^2 \rangle = \frac{1}{2}[2 \pm (e^{i(k_1-k_2).(x_1-x_2)}\langle e^{\pm i(\phi_1+\phi_2-\phi'_1-\phi'_2)}\rangle + c.c.)] \\ &= 1 \pm \cos[(k_1-k_2).(x_1-x_2)]. \end{aligned}$$

The two-particle correlation function can be written as

$$C(k_1,k_2) = \frac{P_2(k_1,k_2)}{P_1(k_1)P_1(k_2)} = 1 \pm \cos[(k_1-k_2).(x_1-x_2)]$$

For extended sources in space and time, if $\rho(x)$ is the normalized space-time distribution, we have

$$\begin{aligned} P_2(k_1,k_2) &= P_1(k_1)P_1(k_2)\int d^4x_1 \int d^4x_2 \, |A(k_1,k_2)|^2 \rho(x_1)\rho(x_2) \\ &= P_1(k_1)P_1(k_2)[1 \pm |\tilde{\rho}(q)|^2], \\ \tilde{\rho}(q) &= \int d^4x \, e^{iq^\mu x_\mu}\rho(x). \end{aligned}$$

Then, the two-particle correlation function can be written as

$$C(k_1,k_2) = \frac{P_2(k_1,k_2)}{P_1(k_1)P_1(k_2)} = 1 \pm \lambda \, |\tilde{\rho}(q)|^2$$

consider the Gaussian profile

$$\rho(x) = e^{-x^\mu x_\mu/(2R)^2} \longrightarrow \rho(q) = e^{-q^2R^2/2} \, .$$

In this very simple example, a typical correlation function is written as

$$C(k_1,k_2) = 1 \pm \lambda \, e^{-q^2R^2}.$$

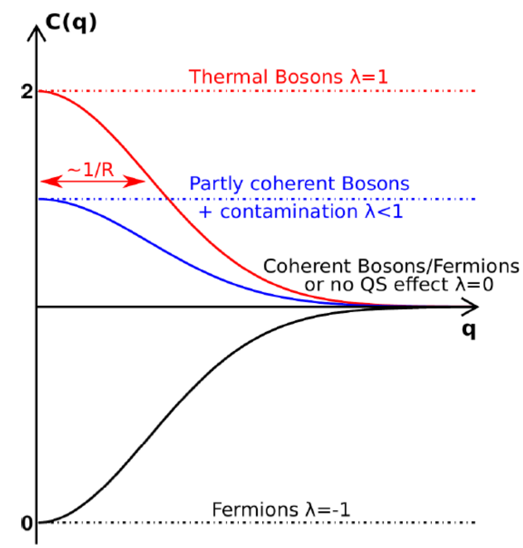

Annu. Rev. Nucl. Part. Sci. 55,357 (2005), Braz. J. Phys. 35 70 (2005), Greifenhagen's PhD thesis (2020).

R_L, R_O and R_S are underestimated at low k_T

a) Treatments on resonance decay (especially long-lived resonance decay). In the low k_T region, the HBT correlation is mainly from the pion from the long-lived Δ resonance decay, and the prescription for resonance lifetimes (especially for broad resonances) used in transport models is still under debate.

b) Non-Gaussian effects. The source radii extracted from the emission source are larger than those extracted from a Gaussian fit to the correlation function.

c) Treatment of the background contribution. This contribution might be from the considerations on the single-track (including particle identification) cuts, collision centrality, reaction plane orientation, and condition of the detector.

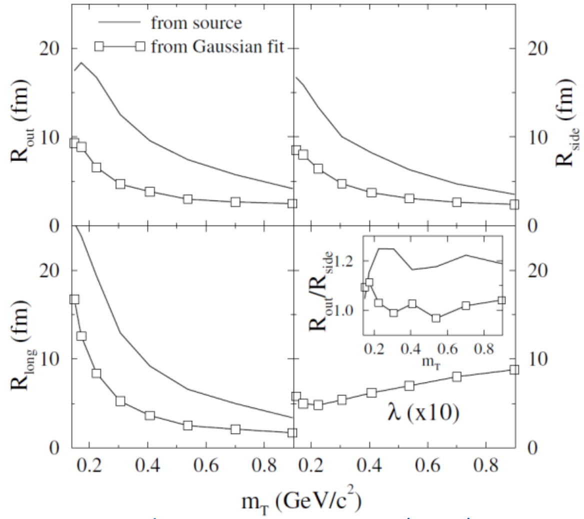

Phys Rev Lett.89.152301(2002).

Annu. Rev. Nucl. Part. Sci. 2005. 55:357–402

Back up

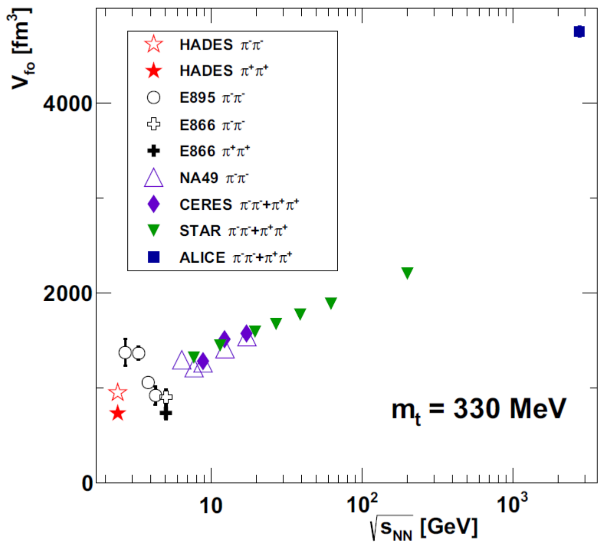

$$V'_{\text{fo}} = (2\pi)^{3/2} R^2_{\text{side}} R_{\text{long}}$$

A non-trivial energy dependence of the source volume V_{fo} is observed at about 4 GeV in experimental data.

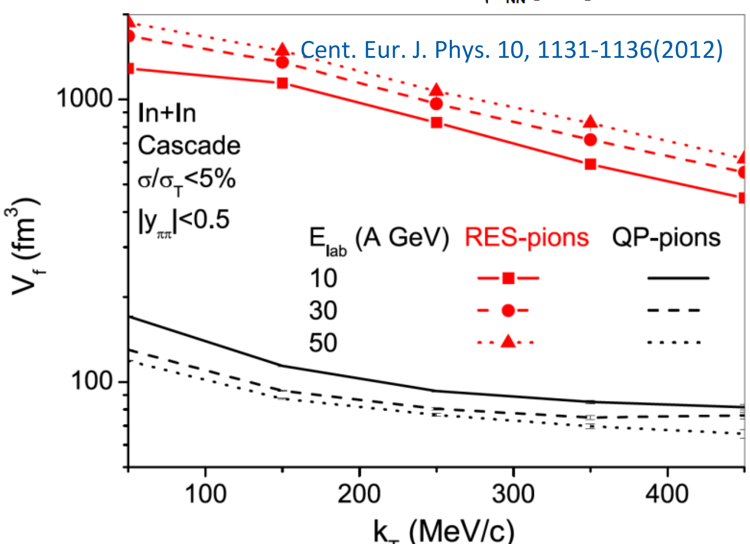

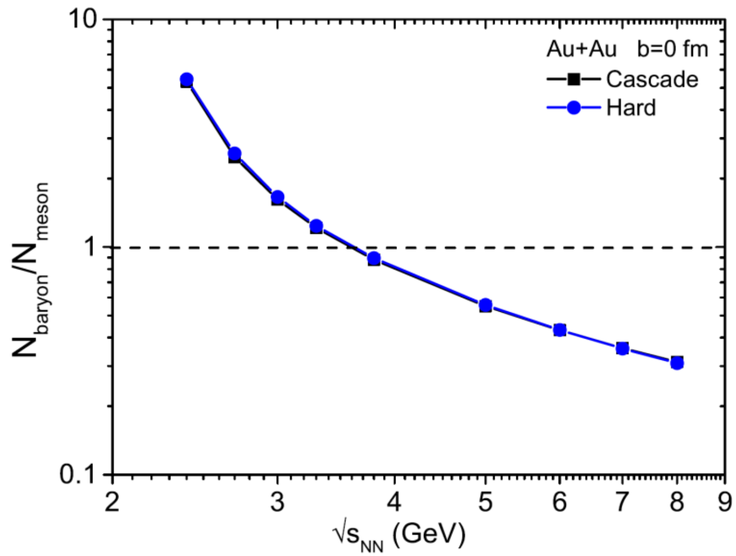

The combination and competition of the resonance decay with the string excitation and fragmentation.

The change from baryon-baryon interaction to meson-meson and meson-baryon interactions.

Resonance decay

case	decay	$\Gamma_{M_\Delta \leqslant M_\Delta^0}$	$\Gamma_{M_\Delta > M_\Delta^0}$
case0	$\Delta_{1232\sim4200}$	$\Gamma(M)$	$\Gamma(M)$
case1	all	$\Gamma(M)$	$\Gamma(M)$
case2	all	Γ	$\Gamma(M)$
case3	all	$\Gamma(M)$	Γ
case4	all	$0.5 * \Gamma(M)$	$\Gamma(M)$

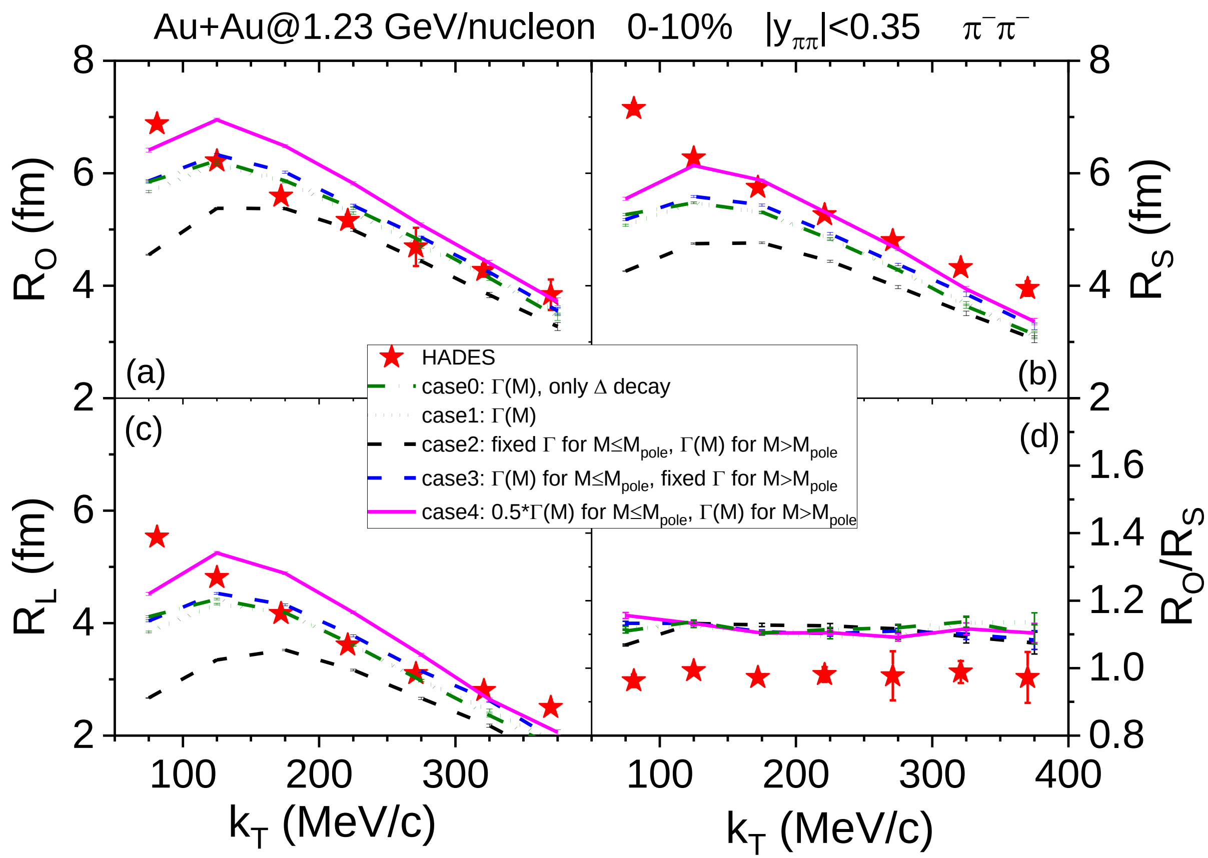

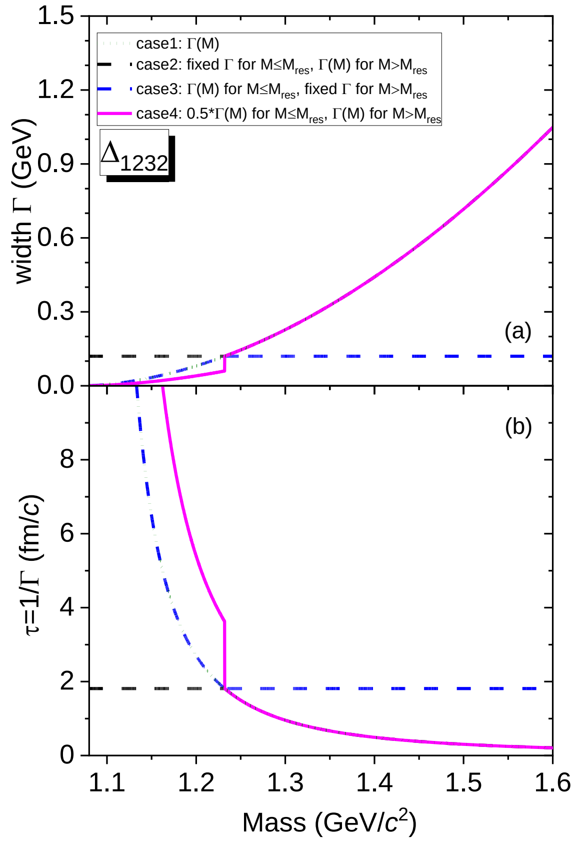

Narrow resonance decay widths (long resonance lifetimes), will decay later and result in a large source.